

Design and synthesis of polyoxometalate-framework materials from cluster precursors

Laia Vilà-Nadal and Leroy Cronin

Abstract | Inorganic oxide materials are used in semiconductor electronics, ion exchange, catalysis, coatings, gas sensors and as separation materials. Although their synthesis is well understood, the scope for new materials is reduced because of the stability limits imposed by high-temperature processing and top-down synthetic approaches. In this Review, we describe the derivatization of polyoxometalate (POM) clusters, which enables their assembly into a range of frameworks by use of organic or inorganic linkers. Additionally, bottom-up synthetic approaches can be used to make metal oxide framework materials, and the features of the molecular POM precursors are retained in these structures. Highly robust all-inorganic frameworks can be made using metal-ion linkers, which combine molecular synthetic control without the need for organic components. The resulting frameworks have high stability, and high catalytic, photochemical and electrochemical activity. Conceptually, these inorganic oxide materials bridge the gap between zeolites and metal-organic frameworks (MOFs) and establish a new class of all-inorganic POM frameworks that can be designed using topological and reactivity principles similar to MOFs.

The molecular design of inorganic materials with porous frameworks is attractive because the process of self-assembly can be harnessed to link small components into larger, functional assemblies^{1,2}. Within the nano-sized pores of these frameworks, control of the chemical environment has been achieved similar to that in molecular capsules, zeolites, micelles and foams³. Zeolites⁴ and metal-organic frameworks (MOFs)^{5,6} are porous materials with regularly repeating holes in their crystal structures that can trap many types of liquid solvents or gas molecules, such as methane or carbon dioxide^{7–10}. By adjusting the size, shape and uniformity of the pores, it is possible to create permeable materials with designed structures (TABLE 1). These structural variations can also exploit hierarchical design principles, such as morphogenesis, self-organization and metamorphosis, which are useful for the development of new synthetic strategies in inorganic materials chemistry¹¹.

Introduction to porous materials

Zeolites. Zeolites are used in a range of applications, including as water softeners, laundry detergents and industrial catalysts for cracking processes, as a consequence of their tunable basicity, ionic nature and robustness¹². Structurally described as framework aluminosilicates,

zeolites consist of linked tetrahedrons of $[\text{SiO}_4]^{4-}$ and $[\text{AlO}_4]^{5-}$. Together, these building blocks form large cavities, and between tetrahedra, the Al and Si atoms are connected by corner sharing of the $[\text{SiO}_4]^{4-}$ and $[\text{AlO}_4]^{5-}$ tetrahedra to form channels in the 3D framework (FIG. 1). These regular arrays of channels and cavities (approximately 3–15 Å) form nanoscale mazes that can trap guest molecules¹³. Additionally, their microporous structures can act as selective catalysts or as adsorbents for molecular mixtures by separating molecules small enough to enter their pores while leaving larger molecules behind.

Although most zeolites have been discovered in the laboratory, they form in nature as a result of the chemical reactions between volcanic glass and seawater or alkaline groundwater at high temperatures ($T > 200^\circ\text{C}$) and pressures ($P > 100\text{ bar}$)¹⁴. For over 2,000 years, zeolites found in volcanogenic sedimentary rocks have been used as stone for the construction of buildings and as a light-weight aggregate in cements and concretes, although their zeolitic nature was recognized only in the 1950s. To date, the International Zeolite Association has recognized 213 zeolitic structures and assigned a three-letter code to each framework topology¹⁵. Zeolites are also commonly classified by pore size, which include pores $< 2\text{ nm}$ (called micropores), pores ranging from 2 nm

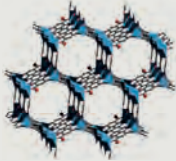
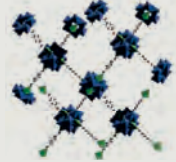
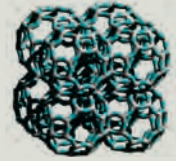
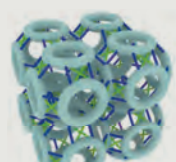
School of Chemistry,
University of Glasgow,
Joseph Black Building,
University Avenue, Glasgow
G12 8QQ, UK.

Correspondence to L.C.
Lee.Cronin@glasgow.ac.uk

doi:10.1038/natrevmats.2017.54
Published online 31 Aug 2017

to 50 nm (called mesopores) and pores >50 nm (called macropores). Their chemical composition is represented by the empirical formula $M_{2/n}O-Al_2O_3-ySiO_2-wH_2O$, where n is the charge of the cation (M), y varies from two to infinity, and w is the number of water molecules contained in the voids of the zeolite. Owing to the trivalent aluminium species, the zeolite has a net negative charge, balanced by the cations hosted in the cage-like cavities. By contrast, pure silicate materials do not contain framework charges because silicon is tetravalent¹⁶. Non-framework cations are often found in the porous network, and their compositions vary. For example, metals from group IA and IIA, such as Na^+ and K^+ , are found in natural zeolites because of the trivalent aluminium species incorporated within the structures.

Table 1 | The diversity of porous materials

Porous materials	Example of structure	Structural diversity	Inorganic content	Ability to delocalize electrons
Metal–organic frameworks (MOFs)	 MOF-74	High	Low	Low
Polyoxometalate-based open frameworks (POM-OFs)	 {MoLa}-based POM-OF	High	Low	Medium
Zeolitic POM-based MOFs (Z-POMOFs)	 Z-POMOF1	Low	Medium	High
Zeolites	 Zeolite A (LTA)	High	High	Low
POM-zeolites (POMzites)	 POMzite-3 (Mn)	High	High	High

Each family of porous materials is shown with a representative structure and an indication of structural diversity, the degree of inorganic content and electronic properties. Bottom image is reproduced with permission from REF. 141, American Chemical Society.

In the 1950s, the first synthetic zeolite was used commercially as an adsorbent. This zeolite — the aluminium-rich Linde type A (LTA) — can be crystallized at temperatures below 100 °C and pH >12. In the 1960s, faujasite (FAU) and mordenite (MOR)¹⁷ became commercially available and were used in catalytic processes in petrochemical refining. For such catalytic applications, the sizes and shapes of the pores are key factors because optimum structural dimensions can increase the selectivity and performance of the catalyst. During this period of zeolite research, control over the structural dimensions of the materials was achieved by tuning the Si:Al ratio in the synthesis. For example, by decreasing the proportion of Si relative to Al, a smaller unit cell can be formed and fewer stabilizing cations are required; hence, the zeolite channels open up. This effect is evident in the sodalite (SOD) zeolite (FIG. 1). By contrast, increasing the Si content relative to Al causes the crystals to be hydrophobic. For example, the aluminium-free Zeolite Socony Mobil-5 (ZSM-5), which is used in the petroleum industry as a heterogeneous catalyst for hydrocarbon isomerization reactions, floats on water¹⁸. An alternative way to achieve control of the structural dimensions is post-synthesis modification of the zeolite¹⁹. The goal of post-synthesis modification is to increase the performance of a zeolite catalyst by controlling the distribution of active sites and their accessibility, poisoning and regeneration. Post-synthesis modifications are an integral part of the zeolite catalyst manufacturing process; the most common methods include thermal activation, ion exchange and chemical vapour deposition²⁰.

In the 1960s–1980s, the search for new zeolite-like structures began to extend beyond traditional aluminosilicates²¹ towards aluminophosphate-based structures. These studies were followed by the exploration of structures containing other elements, such as Be (REF. 22), Zn (REF. 23) and As (REF. 24). By using gallium as a doping agent, gallophosphate cloverite (CLO) was formed, which has a 3D structure with 3 nm-diameter cages accessible through six clover-shaped pores²⁵ (FIG. 1). These cages permit so-called ship-in-a-bottle syntheses for which reagents are small enough to enter through the pores but then assemble into inclusion complexes that are too large to escape the cages²⁶. In such syntheses, the zeolitic crystals are used as micro-sized reactors for the fabrication of templates, enabling platinum-group metal clusters (widely used as catalysts in the petrochemical industry) to be uniformly prepared within the zeolitic porous space.

In the 1990s, research showed that specific pore sizes can also be achieved by the spatially controlled assembly of inorganic building blocks facilitated by cationic or neutral organic molecules. These organic additives act as space-filling molecules around which the zeolite framework forms; hence, they direct the assembly of the structure and balance charges^{19,27}. If the additive drives the reaction towards one particular structure, then the additive is classed as a structure-directing agent, and if the final framework has some of the character of the structure-directing agent, this is described as templating. For example, a specific quaternary amine ($C_{18}H_{36}N^+$) acts as a structure-directing agent in the synthesis of ZSM-18

(REF. 16). Most organic structure-directing agents used in the synthesis of zeolites contain tertiary or quaternary amine nitrogens; the positive charge on the amine balances the negative charge on the zeolite framework^{28–34}. Moreover, new zeolite structures can be developed by designing the template structure²⁹. Another strategy has emerged based on a top-down chemically selective disassembly of a parent zeolite that is subsequently reassembled to form two different framework materials³⁵. This synthetic approach may open pathways to structures that cannot be obtained by standard hydrothermal synthesis.

Metal–organic frameworks. A different approach to prepare microporous solids involves the coordination of metal-containing units — namely, secondary building units — with organic linkers using reticular synthesis to create open crystalline frameworks with permanent porosity³⁶. These framework structures (or MOFs)

have molecular-scale pores (up to 2 nm) and a tunable porous character (FIG. 2). In contrast to zeolites, MOFs have weak thermal and chemical stability owing to the presence of the organic linkers needed to control their geometry and topology³⁷. However, research has shown that MOFs linked by Zr^{IV}-based clusters³⁸ are resistant to methanol, water, acids and bases for a long period of time³⁹. Although there is a need for thermally stable, solvent-resistant and flexible MOFs, discovering new stable inorganic building blocks that would allow a MOF structure to meet those criteria is rare. Porous MOFs are unlikely to compete with zeolites and other oxide-based porous materials in high-temperature applications owing to their limited long-term stability under such conditions and their high cost. However, the ability to prepare these solids, including frameworks with extra-large pores, has opened up applications in new areas. For example, the methane adsorption capacity of MOF-type solids based on copper dicarboxylates and triethylenediamine⁶ exceeds that of any known crystalline material.

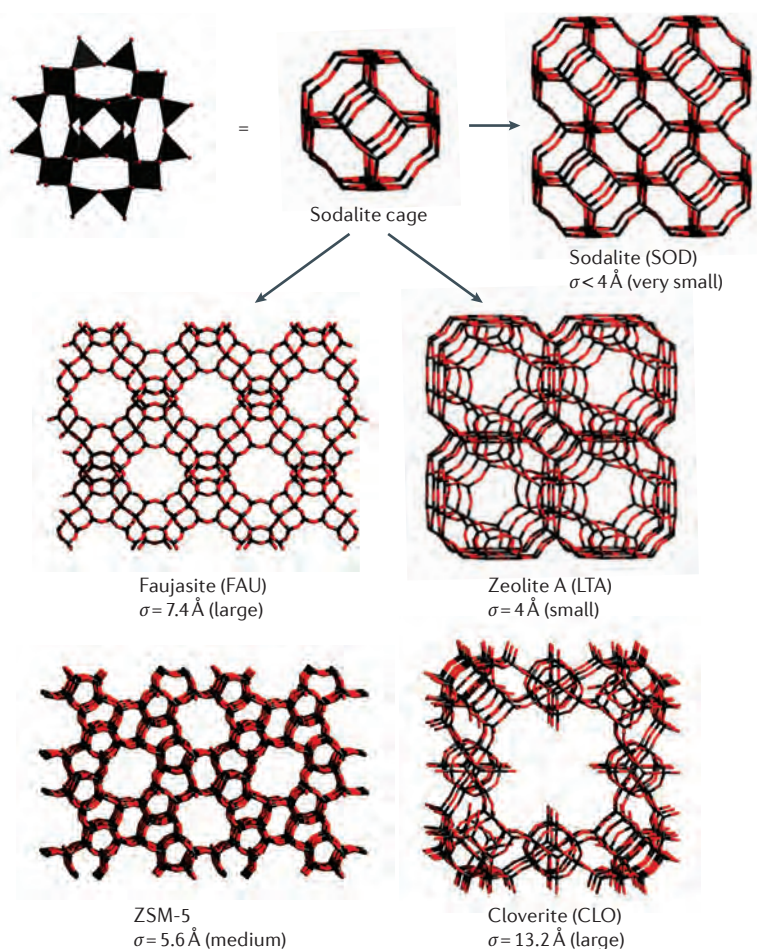


Figure 1 | Schematic illustrations of common zeolite frameworks. The diameter (σ) of the main channels of the zeolites is given in angstroms (\AA). The tetrahedral building blocks form structures known as secondary building units. Sodalite (SOD), faujasite (FAU) and zeolite A (LTA) share the same sodalite unit cell. However, SOD and LTA have cubic arrangements, and FAU is a diamond-like structure of sodalite cages, linked together through the hexagonal faces. Zeolite Socony Mobil-5 (ZSM-5) is composed of pentasil units (eight 5-membered rings in which the vertices are Al or Si) with an O forming a linking bridge between the vertices of the units. The cubic gallophosphate cloverite (CLO) structure has pore openings in the shape of four-leaf clovers. Colour scheme: Si or Al, black; O, red.

Polyoxometalate-based frameworks. Given the incredible diversity of zeolites and MOFs, the approach of synthesizing these materials would be very different if rational design from the ligand to the inorganic framework was possible. In this Review, we discuss how polyoxometalate (POM) clusters can be used as building blocks to design and form framework materials. This is feasible because POMs are discrete (0D) anionic metal oxide molecules, and if these molecules, or fragments of these molecules, can be controllably linked together into frameworks, then this high level of design is possible. The structural diversity and possible connectivity of POMs can result in a range of POM-based frameworks and allow, over time, the elucidation of design principles for the synthesis of specific materials. In solution, POM clusters connect together upon the addition of transition metals or organic moieties, and the structure extends to form coordinatively linked 1D chains, 2D sheets or 3D networks. Indeed, it has recently been shown that POMs can form 3D porous networks, similar to zeolites, if the POMs are in tetrahedral locations and the monodentate Zn-benzenedicarboxylate ligand is used to join the POMs together. These open frameworks are called zeolitic polyoxometalate metal–organic frameworks (called Z-POMOFs)⁴⁰. Moreover, in combination with organic linkers and inorganic cations, POMs can form open frameworks (called POM-OFs) with almost infinite possibilities⁴¹. In a similar vein to MOFs and zeolites, POM-OF materials are porous with high surface areas and thermal stabilities. Last, in combination with transition metal linkers, POMs can form highly stable all-inorganic framework materials; we call these frameworks POMzites to reflect their zeolitic nature and their POM-based constituents (TABLE 1).

Polyoxometalate clusters

POM clusters comprise group 5 or 6 transition metals (V, Nb, Ta, Mo and W) in their highest oxidation states linked by oxygen atoms^{42–53}. These metal–oxygen anionic clusters have been avidly studied over the past two decades, and an increasing number of POM structures are

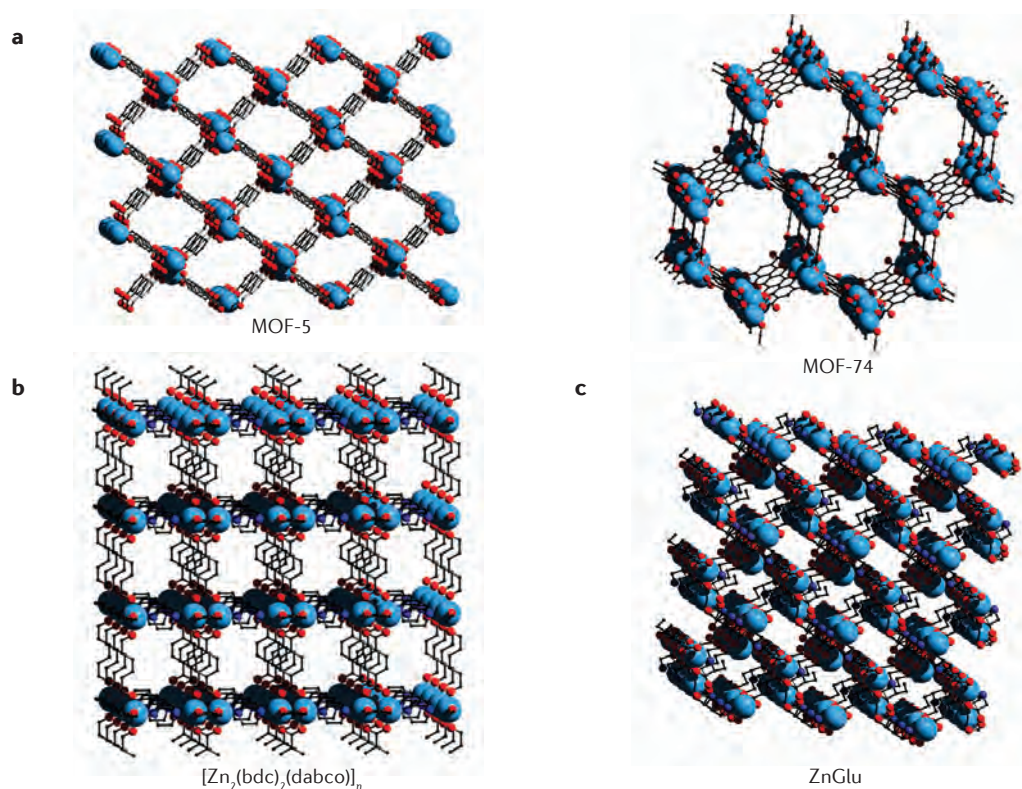


Figure 2 | Metal-organic frameworks comprising Zn₄O clusters and linear organic linkers. **a** | Zn₄O(CO₂)₆ (MOF-5) and Zn₃[(O)₃(CO₂)₃] (MOF-74) contain coordinatively unsaturated Zn(II) sites and secondary building units that are 0D (MOF-5) and 1D (MOF-74). **b** | [Zn₂(bdc)₂(dabco)]_n (bdc = 1,4-benzenedicarboxylate; dabco = 1,4-diazabicyclo[2.2.2]octane) is a typical example of a layer-based MOF with a 2D open framework of Zn₂(COO)₄ paddle-wheel units connected by bdc linkers. **c** | The zinc-glutamate-MOF (ZnGlu), ZnC₅H₇NO₄·2H₂O, is an early example of a MOF structure made from the combination of a first-row transition metal and an organic ligand. Colour scheme: C, black; O, red; Zn, blue; hydrogen atoms omitted for clarity. The structures have been made using the DFT-optimized MOF structures available at <http://dx.doi.org/10.11578/1118280> as a supplement to the CoRE MOF database¹⁴⁶. CoRE, computation-ready, experimental; DFT, density functional theory; MOF, metal-organic framework.

reported each year. Spectroscopic methods, including infrared, resonance Raman, visible and near-infrared, and, in particular, electrospray ionization mass spectroscopy (ESI-MS) and single-crystal X-ray structural analysis, have enabled analysis of the clusters and hence the growth of this research area^{54–56}.

POMs are formed by acidification of alkaline solutions of simple oxoanions. These experimental conditions allow the linking of metal-oxo-based building units via condensation reactions (resulting in the elimination of water). These metal-oxo units can be best seen as metal-centre polyhedra whereby the corners, edges or faces can be shared by metal ions. However, not all of the metal atoms with the ability to form a sixfold octahedral coordination take part in MO₆ linkages: only metals such as Mo^{VI}, W^{VI}, V^V and Nb^V are commonly found in MO₆ units. To form POMs, the metals must meet two requirements: size (octahedral ionic radii ranging from 0.65 to 0.80 Å) and ability to act as a good acceptor of oxygen π electrons. Discrete POM clusters are formed as long as the system is not driven all the way to the infinite oxide structure, which is often the most thermodynamically stable product⁴⁶.

About 82% of the 2,000 most complex structures solved to date and stored in the *Inorganic Crystal*

Structure Database (ICSD) are molybdenum-, tungsten- and vanadium-based POMs⁵⁷. Of these structures, molybdenum-based POM clusters are some of the largest molecular structures elucidated using single-crystal X-ray techniques: these fall into two classes known as Mo-blues or Mo-browns⁴⁶. Mo-browns (Keplerate-type) are spherical clusters based on the {Mo^{VI}₇₂(Mo^V₂)₃₀} structure, where the 30 [Mo^V₂] units can be exchanged for other linkers. By contrast, Mo-blues are gigantic rings with nuclearities of {Mo₁₅₄} or {Mo₁₇₆} (REF. 58). Given the high nuclearity of these clusters, it is not surprising that the second most complex resolved crystal structure, among all resolved crystal structures to date stored in the ICSD, is a molybdenum-based POM containing the spherical polyoxomolybdate cluster of the Keplerate-type {Mo(Mo₅)₁₂(spacer)₃₀}, which has a nanocavity occupied by three concentric shells of water molecules giving a (H₂O)₁₀₀ unit contained within^{57,59}. The structural flexibility of molybdenum-based clusters under reducing conditions is legendary, as shown by the isolation of one of the largest non-biologically derived molecules to date, a lemon-shaped cluster containing 368 molybdenum atoms ({Mo₃₆₈}, the ‘Blue Lemon’)⁶⁰ (FIG. 3). By contrast, the most complex structure reported to date

is the intermetallic compound $\text{Al}_{55.4}\text{Cu}_{5.4}\text{Ta}_{39.1}$, which has great potential as a template for the self-organized growth of complex nanoscale structures^{57,61}.

In a similar manner to corner-sharing zeolites, complex oxide structures, such as $\text{Mo}_2\text{P}_4\text{O}_{15}$, can be formed by corner-sharing metal-centred MoO_6 and PO_4 tetrahedra⁶². $\text{Mo}_2\text{P}_4\text{O}_{15}$, despite its relatively simple chemical formula, has 411 crystallographically unique atoms as a result of this polyhedra corner-sharing network^{57,62}. In the same way, POM structures comprise metal–oxygen polyhedra that are joined through the corner-, edge- and (rarely) face-sharing of oxygen atoms. In fact, the most common building blocks of POMs are metal-centred polyhedra with the general formula $\{\text{MO}_x\}_n$ (where $M = \text{V}, \text{Nb}, \text{Ta}, \text{Mo}$ or W , and x ranges from 4 to 7).

All the POM clusters synthesized so far include anionic multinuclear species with a large range of structures and compositions, and sizes ranging from 1 to 5.6 nm. POMs can be classified into three categories, which are defined by their elemental composition and structure: namely, heteropolyanions, isopolyanions and molybdenum-based clusters (FIG. 3). With only six metal units, the smallest known POM cluster is the isopolyanion called the Lindqvist anion $[\text{M}_6\text{O}_{19}]^{n-}$ (where $M = \text{Mo}, \text{W}, \text{V}, \text{Nb}$ or Ta)⁶³. The other two iconic structures are members of the heteropolyanion family, namely, Keggin⁶⁴ (12 metal-centred $[\text{XM}_{12}\text{O}_{40}]^{n-}$ (where $M = \text{W}$ or Mo ; X is a tetrahedral group, such as $[\text{PO}_4]^{3-}$) and Wells–Dawson⁶⁵ (18 metal-centred $[\text{X}_2\text{M}_{18}\text{O}_{62}]^{n-}$ (where

$M = \text{W}$ or Mo ; X is a tetrahedral group, such as $[\text{PO}_4]^{3-}$) clusters (FIG. 3a). Heteropolyanions include metal oxide cluster shells of tungsten, molybdenum or vanadium that include embedded heteroanions such as $[\text{SO}_4]^{2-}$, $[\text{PO}_4]^{3-}$, $[\text{AsO}_4]^{3-}$ or $[\text{SiO}_4]^{4-}$. The incorporation of a heteroanion offers structural stability to the cluster as well as introducing a negative charge. Tungsten-based structures are the most robust, and their rigidity has been exploited to develop lacunary derivatives — that is, Keggin and Dawson anions with vacancies (most commonly one, two or three vacancies) — that can be linked using electrophiles to form larger aggregates in a predictable manner. The development of lacunary POMs based on Keggin $\{\text{M}_{12-n}\}$ and Dawson $\{\text{M}_{18-n}\}$ is a large research area. Another example of a heteropolyanion is the Preyssler anion (FIG. 3b), which is a cluster with 30 tungsten atoms that connect together to give a large internal cavity⁶⁶.

Isopolyanions are anions that are not associated with a heteroatom or heteroanion and, hence, are less stable than heteropolyanions. As a result, few species have been reported compared with heteropolyanions and molybdenum-based clusters. Isopolyanions have interesting physical properties, for example, high charges and strongly basic oxygen surfaces. Additionally, isopolyanions are often used as prototype model oxide structures to understand physical phenomena associated with the clusters or as building blocks to construct larger structures⁶⁷. Examples of isopolyanions include the Lindqvist anion, the structures of which have the stoichiometry $[\text{H}_x\text{M}_6\text{O}_{19}]^{(8-x)-}$ (where $M = \text{Nb}^{\text{v}}$ or Ta^{v} , and $0 \leq x \leq 3$) and $[\text{M}_6\text{O}_{19}]^{2-}$ (where $M = \text{W}^{\text{vi}}$ or Mo^{vi}). There are several examples of experiments that have relied on the properties of isopolyanions. The nanometre-size Lindqvist-type $[\text{H}_x\text{Nb}_6\text{O}_{19}]^{8-x}$ isopolyoxoanion has been used as a model molecule to study oxygen-isotope exchange reactions for understanding aqueous reactions involving minerals and extended structures, such as the dissolution of oxide materials⁶⁸. Additionally, tungsten Lindqvist anions ($[\text{W}_6\text{O}_{19}]^{2-}$) encapsulated within carbon nanotubes enabled static and dynamic imaging studies to be performed with precision using high-resolution transmission electron microscopy and scanning transmission electron microscopy⁶⁹. More generally, ESI–MS is a useful technique to analyse aqueous solutions of dilute isopolyoxomolybdate⁷⁰ and isopolyoxotungstate⁷¹ systems, resulting in the detection of new isopolyanions. Combining ESI–MS with computational studies helps to elucidate the formation mechanisms of POMs with low nuclearities⁷².

Another interesting example of isopolyoxotungstate is $[\text{H}_4\text{W}_{19}\text{O}_{62}]^{6-}$ $\{\text{W}_{19}\}$ (REF. 73), which was isolated using triethylammonium cations. The structure of the $\{\text{W}_{19}\}$ isopolyanion is a non-classical Wells–Dawson-type cage in which the nineteenth tungsten is located at the centre of the cluster instead of the two tetrahedral heteroatoms that are usually inside conventional Dawson $[\text{X}_2\text{M}_{18}\text{O}_{62}]^{n-}$ clusters. We highlight this structure because it is the first isopolyanion example with a non-classical Wells–Dawson-type cage (the other two examples are heteropolyanions). POM structures often

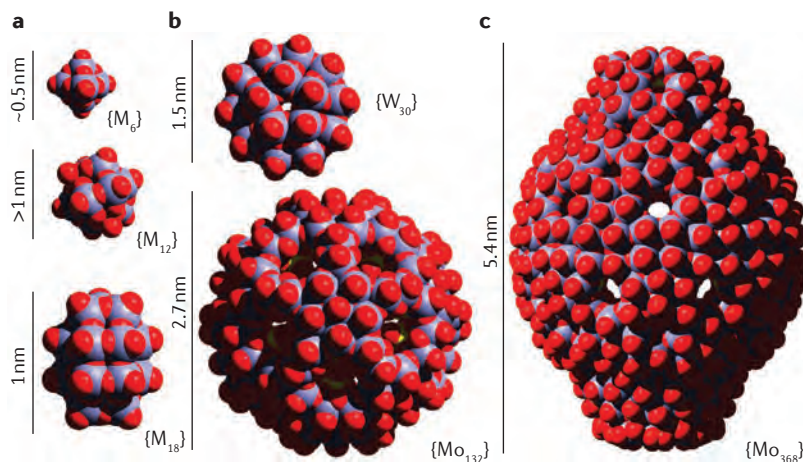


Figure 3 | Structures of polyoxometalate clusters of varying dimensions. **a** | The $\{\text{M}_6\}$ (where $M = \text{Mo}, \text{W}, \text{V}, \text{Nb}$ or Ta) Lindqvist anion $[\text{M}_6\text{O}_{19}]^{n-}$ is formed by the compact arrangement of six edge-sharing MO_6 octahedra (colour scheme: M, lilac; O, red). The $\{\text{M}_{12}\}$ Keggin structure $[\{\text{XO}_4\}_2\text{M}_{12}\text{O}_{36}]^{n-}$ is composed of four M_3O_{13} groups of three edge-sharing MO_6 octahedra, which are linked together by sharing corners and connecting to the central XO_4 tetrahedron. The $\{\text{M}_{18}\}$ Wells–Dawson structure $[\{\text{XO}_4\}_2\text{M}_{18}\text{O}_{54}]^{n-}$ (where X is such that a tetrahedral group is formed, such as $[\text{PO}_4]^{3-}$) can be seen as two fused Keggin fragments. **b** | The $\{\text{W}_{30}\}$ Preyssler anion $[\text{X}^{\text{v}}\text{P}_5\text{W}_{30}\text{O}_{110}]^{(15-n)-}$ has an internal cavity that can be occupied by different cations (for example, Na, Mn or Eu). The Keplerate-type structure $\{\text{Mo}_{132}\}$ forms as a result of spherical disposition of pentagonal $\{(\text{Mo})\text{Mo}_3\}$ building blocks (S, yellow). **c** | The largest cluster to date is the lemon-shaped $\{\text{Mo}_{368}\}$, which comprises 368 metal (1,880 non-hydrogen) atoms and forms by the linkage of 64 $\{\text{Mo}_3\}$, 32 $\{\text{Mo}_2\}$ and 40 $\{\text{Mo}(\text{Mo}_3)\}$ units. The polyoxometalate clusters in panels **a–c** are to scale and show the wide range of sizes that are possible.

present isomerism, and, in this particular case, two isomers α - and γ^* -[H₄W₁₉O₆₂]⁶⁻ were characterized crystallographically. The α form has *D*_{3h} symmetry, and the γ^* form has *D*_{3d} symmetry. In fact, {W₁₉} was used as a model to understand the likely reactivity and electronic structure of POMs⁷⁴ and as a control molecule for memory device experiments⁷⁵.

Reduced molybdenum-based POM clusters were described by Scheele in 1783, who reported the blue colour of acidified molybdenum salts. Their composition was unknown until the synthesis and structural characterization in 1995 of the very high nuclearity {Mo₁₅₄} cluster⁵⁸. This {Mo₁₅₄} cluster crystallized from a solution of Mo-blue, and X-ray crystallography revealed a 3.6 nm ring structure. By understanding the experimental conditions that govern molybdenum reactions, the first member of the Mo-brown species, {Mo₁₃₂}, was discovered and shown to have a porous spherical topology⁷⁶. One of the components of {Mo₁₃₂} is the pentagonal {Mo(Mo)₅} unit, which is pivotal for connecting the building blocks to form closed structures, such as those found in many of the spherical Mo-blue and Mo-brown structures. These {Mo(Mo)₅} building blocks, in the presence of suitable linkers, such as doubly bridging {MoV₂O₄(ligand)} units, where the ligand is, for example, acetate or sulfate, lead to giant mixed-valence clusters with diverse topologies. Examples of these giant clusters are the spherical icosahedral {Mo₁₃₂} (FIG. 4), big wheel {Mo₁₅₄} and {Mo₁₇₆}, capped cyclic {Mo₂₄₈} and basket-shaped {Mo₁₁₆} architectures⁷⁷.

Derivatizing polyoxometalate clusters

Transition metal oxides show interesting phenomena, from superconductivity to magnetoresistance and multiferroicity, making them vital components of current and future technologies. In these cases, these metal oxides are attractive because their chemical and

electronic properties can be tuned by varying the constituents of the material. Their properties are determined by how quantum clouds of electrons — the orbitals — move around and interact with each other⁷⁸. Hence, by thoughtfully combining transition metal oxides with other molecules or metals, it is possible to tune the properties of the materials. To develop new materials, it is important that their precursors are easily synthesized and derivatized in good yields, which is key if POM clusters are to be derivatized to form new materials. Making derivatives is difficult because the synthesis of POMs is commonly achieved under simple one-pot conditions that lead to the formation of complex mixtures, which are mainly governed by self-assembly mechanisms. This implies that a slight variation in the reaction conditions (for example, a change in pH or temperature) can easily result in the formation of different cluster architectures. In some cases, chance seems to govern the discovery of clusters, and despite the observation of some general speciation rules, the resulting architectures cannot always be predicted. However, POM structures, once identified, can be used as building blocks in the formation of other materials once the synthesis has been reliably mastered.

Lacunary clusters formed by the hydrolysis of parent anions — for example, the Keggin anion [SiW₁₂O₄₀]⁴⁻ or Dawson anion [P₂W₁₈O₆₂]⁶⁻ — can be functionalized in a controlled manner. In the case of the Keggin anion, lacunary clusters, such as [SiW₁₁O₃₉]⁸⁻ or [SiW₁₀O₃₄]⁸⁻, are formed, which have one or two vacant coordination sites, respectively. These vacant sites can be functionalized with metal cations, giving POM clusters such as [M(H₂O)SiW₁₁O₃₉]ⁿ⁻ and [(M(H₂O))₂SiW₁₀O₃₄]ⁿ⁻ (where M is a metal cation). In particular, the dilacunary polyoxoanion [γ -SiW₁₀O₃₆]⁸⁻, denoted as [γ -SiW₁₀], exists in more isomeric forms than any other known lacunary polyoxoanion. For this reason, [γ -SiW₁₀] is a commonly used, structurally flexible precursor in POM chemistry and has been used to make a library of metal-functionalized POMs⁷⁹. Among these, the most common stoichiometries are {SiW₈} (REF. 80,81), {SiW₉} (REF. 82), {SiW₁₀} (REF. 83) and {SiW₁₁} (REF. 79). By combining the lacunary K₈[γ -SiW₁₀O₃₆] with transition metals, such as Mn, Cu and Ti, it has been possible to make high-nuclearity transition metal-substituted POM clusters, for example, {Cu₁₄Si₄W₃₂} (REF. 80), {Mn₁₉Si₆W₆₀} (REF. 84), {Mn₁₀Si₄W₃₆} (REF. 85), {Ti₈Si₄W₄₀} (REF. 86), {Mn₆Si₃W₂₇} (REF. 87), {Ni₆P₂W₁₅} (REF. 88) and a Zr₂₄-cluster substituted poly(polyoxotungstate)⁸⁹.

Another example of the diversity of silicotungstate derivatives is {Ru₄Si₂W₂₀}, which has emerged as a highly promising catalyst for water oxidation⁹⁰ and has been extensively studied⁹¹. Remarkably, [γ -SiW₁₀] has been reported as a precursor for the epoxidation of olefins⁹² and has been used to obtain single-molecule magnets⁹³. Further interesting properties of silicotungstate derivatives include the formation of self-assembled monolayers on Ag(111)⁹⁴ and of Pt-substituted structures that have the potential to be used as catalysts⁹⁵. From a mechanistic point of view, the transformation of the lacunary polyoxoanion [β_2 -SiW₁₁O₃₉]⁸⁻ into [γ -SiW₁₀O₃₆]⁸⁻ has

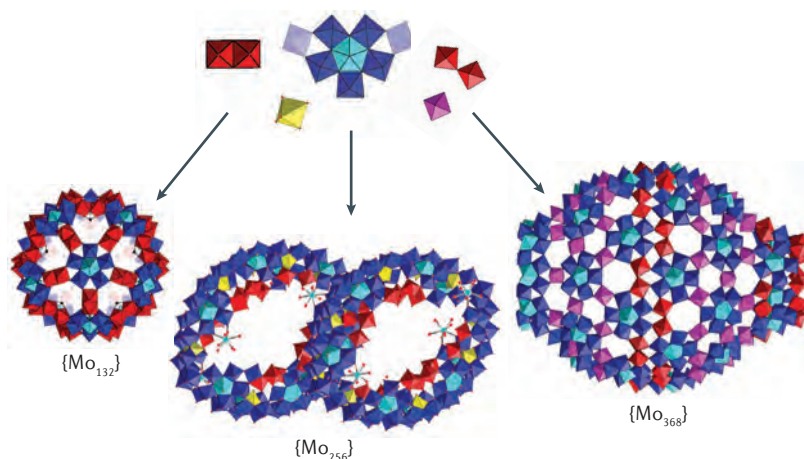


Figure 4 | Comparison of the molecular sizes and building blocks of {Mo₁₃₂}, {Mo₂₅₆} and {Mo₃₆₈} clusters. In each structure, the building blocks are shown as coloured polyhedra. In the {Mo(Mo)₅} units, the outer five {Mo₁} units are dark blue, and the inner 5-fold Mo unit is cyan. There are two types of {Mo₂} (corner- and edge-sharing links, shown in red) and three types of {Mo₃} (pale blue, yellow and pink). The corner-sharing {Mo₂} units are in the wheel {Mo₂₅₆} and lemon, and the edge-sharing {Mo₂} units are in the ball. Figure is reproduced with permission from REF. 77, Royal Society of Chemistry.

intrigued the POM community for decades. Through the use of ESI–MS data and theoretical calculations, it has been shown that the reaction proceeds through an unexpected $\{\text{SiW}_6\}$ precursor capable of undergoing a direct $\beta \rightarrow \gamma$ isomerization via a rotational transformation⁹⁶. This finding is a step towards understanding the mechanism of the assembly of POMs.

Until the late 1990s, the controlled functionalization of POMs was limited to tungsten-based^{97,98} and molybdenum-based lacunary clusters, and there were no synthetic strategies for vanadium-based clusters⁹⁹. However, the likelihood that the controlled design of polyoxovanadates would offer active materials for energy conversion, (photo)catalysis and molecular magnetism has promoted research efforts in this area. With this motivation in mind, a method has been developed that allows the reactivity of vanadium oxide clusters to be tuned by functionalization with certain metals. More specifically, dimethylammonium acts as a hydrogen-bonding cation and is used as a molecular placeholder to block metal-binding sites within the vanadium-based clusters. Subsequent stepwise replacement of the placeholder cations with reactive metal cations gives monofunctionalized and difunctionalized clusters¹⁰⁰.

Another example of the controlled functionalization of POMs is the formation of two polyoxotungstates with the general formula $[\text{M}_6(\text{PW}_6\text{O}_{26})(\text{P}_2\text{W}_{15}\text{O}_{56})_2(\text{H}_2\text{O})_2]^{23-}$ ($\text{M} = \text{Co}^{\text{II}}$ or Mn^{II}), which contain $\{\text{PW}_6\}$ fragments generated from the $[\text{P}_2\text{W}_{15}\text{O}_{56}]^{12-}$ precursor. These polyoxotungstates are made by the transformation of a Dawson lacunary cluster into a Keggin lacunary building block¹⁰¹. In this case and in other similar experiments, analysis of the reaction mixture by ESI–MS has been used to follow the incorporation of non-conventional phosphorus^{III}-based anions into a POM cage. For example, the self-assembly of two phosphite anions $[\text{HPO}_3]^{2-}$ in a $\{\text{W}_{18}\text{O}_{56}\}$ cage can be followed by ESI–MS and NMR spectroscopy during the formation of the tungsten-based unconventional Dawson-like cluster, $[\text{W}_{18}\text{O}_{56}(\text{HPO}_3)_2(\text{H}_2\text{O})_2]^{8-}$. These techniques were used to elucidate the structural rearrangement of the cluster building blocks in solution and clarify the mechanism by which the $\{\text{HPO}_3\}$ moieties dimerize to form weakly interacting ($\text{O}_3\text{PH}\cdots\text{HPO}_3$) moieties¹⁰².

The modification of POMs to incorporate terminal alkyne and azide groups and the development of appropriate conditions for their Cu-catalysed alkyne–azide cycloaddition (or click reaction) have been achieved. By combining reaction control and minimizing side products, it is possible to make various oligomeric POM clusters, ranging from two to five clusters in length, in high yields and high purities. This high degree of structural control yields hybrid organic–inorganic oxides (approximately 4–9 nm in diameter) with molecular weights ranging from 2 to 10 kDa (REF. 103).

Choosing the optimum counterion is not trivial in most POM syntheses. In the case of the iron-oxo cluster, $\alpha\text{-}[\text{FeO}_4\text{Fe}_{12}\text{O}_{12}(\text{OH})_{12}(\text{O}_2\text{C}(\text{CC}_{13})_{12})]^{17-}$, termed the Fe_{13} ion, the choice of counterion has proven to be particularly important. In fact, the stabilization

of highly reactive Fe_{13} , which has a 1 nm discrete Keggin structure, has only been possible by using Bi^{III} (REF. 104). Considering iron POM chemistry more generally, the following isomeric anions have been isolated from the same experimental conditions: $[\text{Fe}^{\text{III}}(\text{H}_2\text{O})_2\{\gamma\text{-Fe}^{\text{III}}\text{SiW}_9\text{O}_{34}(\text{H}_2\text{O})_2\}]^{11-}$ and $[\text{Fe}^{\text{III}}(\text{H}_2\text{O})_2\{\gamma\text{-Fe}^{\text{III}}_2\text{SiW}_8\text{O}_{33}(\text{H}_2\text{O})_2\}\{\gamma\text{-SiW}_{10}\text{O}_{35}\}]^{11-}$ (REF. 105). The simple nature of these synthetic systems, involving just Fe^{II} and $\{\gamma\text{-SiW}_{10}\}$ salts at a certain pH, enables analysis of the reaction by time-resolved ESI–MS. This investigation yields informative mechanistic details regarding the initial interactions and reorganizations of the $\{\gamma\text{-SiW}_{10}\}$ precursor and Fe^{II} (REF. 105).

Another example of structural control is clusters that incorporate redox-active anions (FIG. 5). These non-classical Dawson clusters, with the general formula $[\text{H}_n\text{M}_{18}\text{O}_{56}(\text{XO}_6)]^{m-}$ (where $\text{X} = \text{W}^{\text{VI}}$, Te^{VI} or I^{VII}), embed an octahedral or trigonal prismatic redox-active template within the cluster shell^{106,107}, namely, $\{\text{W}_{18}\text{O}_{56}\text{XO}_6\}$. Non-classical Dawson clusters (where $\text{X} = \text{I}^{\text{VII}}$ or Te^{VI}) with a localized redox-active template have been synthesized, and their redox properties have been compared with the pure tungsten control ($\text{X} = \text{W}^{\text{VI}}$). In the tungsten control, the reduced electron is delocalized, but in the I or Te clusters, the reduced electron is localized on the heteroatom, giving I^{VI} or Te^{V} , respectively⁷⁴. Two recent examples of tuning the assembly of POM network structures are the $[(\text{P}^{\text{V}}\text{Mn}^{\text{II}}\text{W}^{\text{VI}})_{11}\text{O}_{39}]_2[\text{P}^{\text{V}}\text{O}_4]^{13-}$ and $[\text{P}_2\text{Mn}_4\text{W}_{18}\text{O}_{68}]^{10-}$ clusters, synthesized from the same reaction mixture with only a slight variation in pH and temperature¹⁰⁸. Finally, another example of structural control is the synthesis of the tetrameric $[\text{Se}_8\text{W}_{48}\text{O}_{176}]^{32-}$ wheel¹⁰⁹, whose stability in solution was probed by ESI–MS.

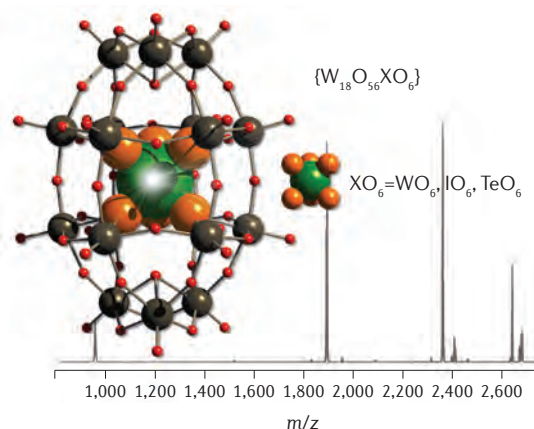


Figure 5 | Characterization of the non-classical Wells–Dawson $\{\text{W}_{18}\text{O}_{56}\text{XO}_6\}$ cluster. X-Ray and electrospray ionization mass spectrometry studies exploring the formation of redox-active polyoxometalate clusters with redox-active heteroanions developed from the parent $\{\text{W}_{18}\text{O}_{56}\text{XO}_6\}$ cluster. The mass spectrum shows Dawson-like clusters ($\text{X} = \text{I}^{\text{VI}}$, Te^{VI} or W^{VI}) have been synthesized thus providing new redox-active units for the development of materials. Colour scheme: W, grey; O, red; oxo of the XO_6 , orange; X, green. Figure is reproduced with permission from REF. 147, Royal Society of Chemistry.

Polyoxometalate-based open frameworks

Mixing POMs with large organic cationic coordination compounds is an easy way of forming large hybrid salt structures with nanoscale porosity. These structures show characteristic properties associated with the configuration of their pores, the type of POM and the type of metal atom in the POM. The combination of organic linkers and POMs results in the formation of extended structures similar to MOFs but with much less control of the eventual structure. These hybrid salt structures have been termed POM-based open frameworks (POM-OFs)⁴¹. The selection of cationic and anionic components determines the structure and properties of POM-OFs. For example, the ratio of cation/anion, which can be controlled by the charge on both components, affects the sorption properties of the resultant POMs. In the case of the Dawson-type POMs, $[\alpha\text{-P}_2\text{W}_{18}\text{O}_{62}]^{6-}$, $[\alpha_2\text{-P}_2\text{W}_{17}\text{V}_1\text{O}_{62}]^{7-}$ and $[\alpha\text{-P}_2\text{W}_{15}\text{V}_3\text{O}_{62}]^{9-}$ combined with the large cation (for example, $[\text{Cr}_3\text{O}(\text{OOCH})_6(\text{H}_2\text{O})_3]^{+}$), ionic crystals with different sorption properties for ethanol, methanol and water molecules are formed. The voids in the crystal are proportional to the charge of the anion; more specifically, the larger the anion charge, the smaller the void¹¹⁰. In another example, if the cation comprises pendant alkyl chains ($[\text{Cr}_3\text{O}(\text{OCC}_2\text{H}_5)_6(\text{H}_2\text{O})_3]^{+}$), the hydrophobicity of the pores increases¹¹¹. Finally, if the anion in the dodecatungstophosphate $\text{M}_3\text{PW}_{12}\text{O}_{40}$ is changed (for example $\text{M} = \text{Cs}, \text{NH}_4$ or Ag), the surface area and the porosity of the nanocrystallites increase¹¹².

Heterometallic POM anions, such as $\{\text{M}(\text{OH})_2\}_2\{\mu_3\text{-OH}\}_2\{\text{Zn}(\text{OH})_2\}_2$ ($\text{M} = \text{Co}, \text{Ni}$ or Zn), combined with tetrabutylammonium cations form porous ionic crystals with large void volumes (between 38 and 58 Å³) that encapsulate mobile guest molecules¹¹³ (FIG. 6). For example, a highly porous material with a cubic arrangement of $\{\text{V}_{18}\}$ cages interconnected through either Fe or Co bridging units allows the interpenetration of two frameworks¹¹⁴, which is a common phenomenon in MOF chemistry. Additionally, a POM-OF containing

Wells–Dawson clusters linked through Ni^{II} cations, with chelating 1,3-bis(4-pyridyl)propane ligands completing the coordination sphere of the Ni^{II} centres, has been prepared. The organic ligands prevent the interpenetration of the cage and help to retain the porous nature of the framework¹¹⁵. This combination of a highly flexible nitrogen donor ligand (1,3-bis(4-pyridyl)propane) with NiCl_2 and $[\alpha\text{-P}_2\text{W}_{18}\text{O}_{62}]^{6-}$ Wells–Dawson cluster produces a perovskite-type structure, indicating that POMs can be arranged into zeotype frameworks. Until the early 2000s, the assembly of POM-OF units with high symmetry and control was not possible. However, by understanding the localized molecular reactivity on the oxygen-rich surfaces of POM clusters, it has become possible to generate reactive building blocks that can enable the discovery of new pure inorganic frameworks, because cluster-based nodes of a given symmetry can be reliably generated. Hence, all-inorganic structures can be fabricated that go beyond what has been proposed for the formation of POM-OFs¹¹⁶.

Some examples of POM-OFs are reported in the following section. Here, we start with a strategy to build soft, single-layer, ionic organic–inorganic 2D frameworks. These frameworks are held together by electrostatic interactions; however, there is no preferred direction of the bonding. This has been achieved by means of an ionic self-assembly of bridging cations of α -cyclodextrin-based pseudorotaxanes with anionic $[\text{PW}_{11}\text{VO}_{40}]^{4-}$ cluster nodes in water¹¹⁷. The supramolecular frameworks obtained have uniform and adjustable ortho-tetragonal nanoporous structures with pore sizes ranging from 3.4 to 4.1 nm, and are promising for applications in selective ion transport, molecular separation and dialysis systems. More importantly, the introduction of $[\text{PW}_{12}\text{O}_{40}]^{3-}$ into a porous cationic framework has proven to be a successful strategy to enhance the proton conductivity of ionic-based materials¹¹⁸. This approach mimics the proton-conducting mechanism of Nafion films, which are used in fuel cells and electronic devices, and can be used to construct a low-cost high-proton-conductive alternative material that can be used at higher temperatures than those possible with Nafion films (above 80 °C).

Two POM-OFs, in which the POM fragments serve as nodes and are directly connected with organic ligands, can be combined to give 3D open frameworks¹¹⁹. The crystal surfaces of these POM-OFs can be modified using pyrrole or aniline as monomers. This approach leads to the formation of the corresponding polymers by an oxidative polymerization process initiated by the redox-active POM scaffolds. Guest-exchange experiments demonstrate that the guest-exchange rate can be tuned by a variation in the structure or composition of the polymers, and the structural integrity of the framework is retained after surface modification.

Solvothermal synthetic methods are used to obtain a decatungstate-based MOF with a 1D structure type. This method offers an environmentally friendly route for widening the scope of accessible nitriles in both the laboratory and industry¹²⁰. Also, solvothermal synthesis has enabled the encapsulation of POMs within the large

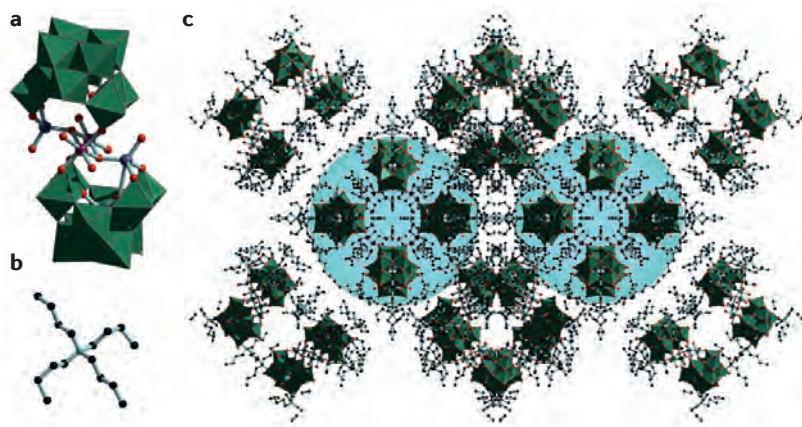


Figure 6 | A highly porous ionic crystal. a, b | The ionic crystal comprises the $[\text{Co}_2\text{Zn}_2\{\text{SiW}_{10}\}_2]$ sandwich polyoxometalate anions (part **a**), combined with tetrabutylammonium cations (part **b**)¹¹³. **c** | This structure contains spherical $38 \times 38 \times 38 \text{ \AA}^3$ cavities (indicated by blue spheres), in which the guest molecules are highly mobile and may be exchanged. All hydrogen atoms and solvent molecules are omitted for clarity. Colour scheme: W, green polyhedra; O, red; C, black; N, blue; Zn, dark grey; Co, purple.

pores of Zr^{IV} biphenyldicarboxylate UiO-67 MOF¹²¹, whereby the POMs can themselves be used as guests and templates for MOF structures. Mo^{VI} oxide hybrid POM-OFs have also been synthesized under mild hydrothermal conditions or by refluxing in water. These compounds exhibit interesting catalytic activities and are able to trap several different solvents^{122,123}. Other examples include the iron Keggin ion that has been identified as a structural building block in both magnetite and ferrihydrite, which are two common iron oxide phases in nature and technology. Discrete molecular forms of the iron Keggin ion that can be manipulated in water or chemically converted to the related metal oxides are important for understanding the mechanism of growth, in particular, non-classical nucleation, in which cluster building units are preserved during aggregation and condensation processes. In fact, two isomeric Keggin ions¹²⁴ (the lacunary α_1 -[PW₁₀O₃₇]⁹⁻) with the assistance of pyridazine bridges, can be used to form a sandwiched Co^{IV}-POM cluster compound¹²⁵.

Organic metalloporphyrins and inorganic POMs have been used as active moieties for the synthesis of porous materials to realize highly efficient heterogeneous catalysis¹²⁶. Vanadium POMs have been successfully used to expand the POM-OF family. For example, a decavanadate-based microporous POM-OF structure has been shown to have covalent decavanadate metal-organic layers with square voids. The stacking of these voids is aided by interlamellar cementing complexes and generates water-filled channels with cross-sections ranging from 8.8 to 10.4 Å (REF. 127). Another framework structure is composed of fully reduced cyclic {V₆N₆O₁₈}, which adopts an Anderson-like structure, linked together with six triethanolamine ligands to form a 3D network¹²⁸. Although POM-OFs are an attractive area in terms of searching for new structures, the problems associated with MOFs in relation to their stability are likely to be exacerbated with POM-OFs because of the weak interactions between charges in the lattice and the many possible configurations of bridging ligands. Also, the explosive increase in the number of structures is problematical because there is no well-established taxonomy to help guide the interested synthetic chemist.

All-inorganic polyoxometalate frameworks

To make all-inorganic POM-framework materials comparable with zeolites, it is not possible to use organic cations or coordination complexes that are also linking cations. To make such materials, highly charged POM building blocks that can coordinate with transition metal ions without supporting organic chelating ligands must be obtained. For example, the cyclic heteropolyanion, [P₈W₄₈O₁₈₄]⁴⁰⁻ (abbreviated as {P₈W₄₈}), is an ideal building block for the construction of porous framework materials, and a number of coordination polymers incorporating this POM ligand have been prepared^{129,130}. The assembly of frameworks needs not only a well-defined POM cluster or pro-cluster (that is, a cluster that will undergo a rearrangement reaction to form the desired synthon), but also a first-row transition metal linker with weak ligands to engineer reactions. This type of linker enables

the anionic POM cluster building block to displace the ligands and ensures the formation of coordination bonds between the transition metal and the cluster-oxo POM. This approach has been used to assemble coordinatively linked 1D chains, 2D sheets and 3D networks^{40,98,131,132} with POM cluster building blocks. Similar to MOFs, these purely inorganic networks have properties that are tunable through rational synthetic design whereby a cluster with the intrinsic property can be used to form a framework with that corresponding property^{133,134}.

The incorporation of POM guests inside porous frameworks that can recognize the acidic, electronic and catalytic properties of these clusters may enhance the overall framework structure¹³²⁻¹³⁴. In particular, the crown-type heteropolyanion {P₈W₄₈} is notable for several properties, including its highly negative charge and remarkable electrochemistry¹³⁵⁻¹³⁸. Its intrinsic nanometre-sized cavity means {P₈W₄₈} is an ideal candidate to be used as a synthon to prepare open-framework materials with microporosity^{134,138-140}. Such structures have been prepared by adding first-row transition metals to aqueous solutions of {P₈W₄₈} (REFS 140,141) (FIG. 7). Moreover, it is possible to control the structure of these {P₈W₄₈}-based porous frameworks by altering the reaction conditions, and the classification of this family using a new type of taxonomy has been proposed. This structural diversity arises because the exo-cyclic coordination of first-row transition metals to {P₈W₄₈} typically yields frameworks that extend through {W-O-transition metal-O-W} bridges in 1D, 2D or 3D, and these bridging types can be controlled by the transition metal and synthetic conditions (for example, pH or co-solvent).

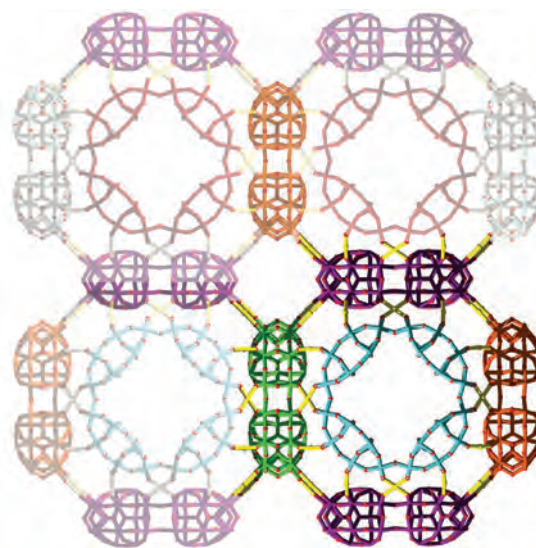
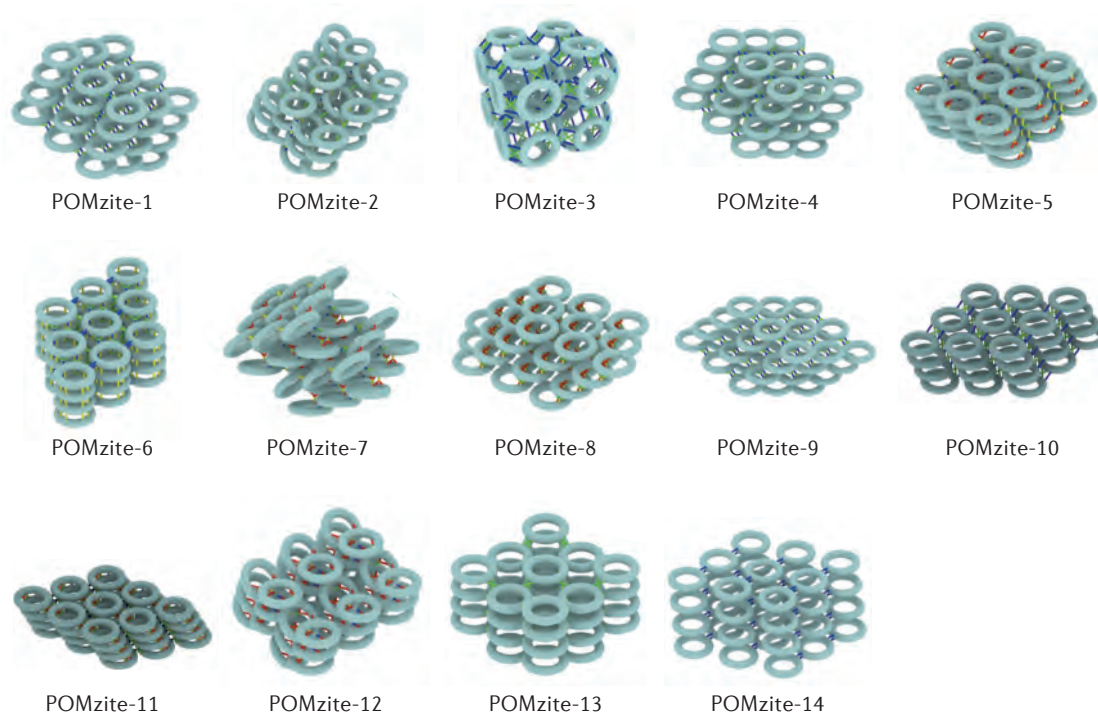


Figure 7 | A polyoxometalate open framework material. The polyoxometalate open framework (POM-OF) [Mn₈(H₂O)₄₈P₈W₄₈O₁₈₄]²⁴⁻ forms a porous structure that is built from the face-directed assembly of highly anionic [P₈W₄₈O₁₈₄]⁴⁰⁻ molecular building units (cyan, purple, green and orange), electrophilic manganese linkers (yellow) and oxo ligands (red). The anionic units are ring structures with pores of 1 nm in diameter, and the manganese linkers are redox switchable.

Using $\{P_8W_{48}\}$ as a building block, more than 30 zeolite-like POM frameworks have been reported since 2009, suggesting that POM-zeolites or POMzites represent a new family of inorganic frameworks (FIG. 8). So far, 14 unique POMzite architectures have been observed and numbered chronologically according to their date of publication¹⁴¹. Despite the similarities of

POMzites and zeolites in terms of their composition and properties, these families are accessed via contrasting routes of assembly. More specifically, POMzites are prepared in a modular manner, whereas zeolites are typically synthesized using a one-pot method. This modular approach is valuable because it allows greater control over the eventual topologies of the POMzites, and this



Code	Transition metal	Type of structure	Year of publication
POMzite-1	Co or Mn	Chain	(Co) 2009 (REF. 148) (Mn) 2017(REF. 141)
POMzite-2	Co	Herringbone ¹⁴⁸	2009
POMzite-3	Mn	Cube ¹³⁴	2010
POMzite-4	Co	Chain ¹⁴⁹	2010
POMzite-5	Co or Ni	Column ¹⁵⁰	2010
POMzite-6	Mn	Column ¹⁵¹	2011
POMzite-7	Mn	Herringbone ¹⁵¹	2011
POMzite-8	Mn	Column ¹⁵²	2011
POMzite-9	Mn	Chain ¹⁵²	2011
POMzite-10	Co	Chain ¹⁴⁰	2017
POMzite-11	Co	Column ¹⁴⁰	2017
POMzite-12	Co	Herringbone ¹⁴⁰	2017
POMzite-13	Mn	Column ¹⁴¹	2017
POMzite-14	Ni	Chain ¹⁴¹	2017

Figure 8 | A numbering system for known POMzites. The transition metals and the type of structure, including chain (1D), column (2D), herringbone (3D) or cube (3D), of the POMzites are noted. POMzites, all-inorganic framework materials with zeolitic nature and polyoxometalate-based constituents. Images are reproduced with permission from REF. 141, American Chemical Society.

control enables the precise tuning of these materials for tailored applications.

Although it is not yet clear if POMzites could lead to compounds as diverse and useful as zeolites, it is important to explain why these compounds are unique and interesting. To do so, we discuss a recent example of a POMzite made by linking inorganic rings of the tungsten oxide $\{P_8W_{48}\}$ building block¹⁴¹. This yields POMzite crystals that can undergo at least eight different crystal-to-crystal transformations, with gigantic crystal volume changes ranging from $-2,170$ to $+1,720 \text{ \AA}^3$ and no reduction in crystallinity¹⁴⁰. This material shows the largest change in volume for a single crystal-to-single crystal transformation reported to date. The crystal also shows conformational flexibility while maintaining robustness over several cycles of reversible uptake and release of guest molecules, such as NH_3 , H_2O and CH_3OH , and switching of the crystal between eight different metamorphic states. The parent compound, $\text{Li}_9\text{K}_7\text{W}_1\text{Co}_{10}[\text{H}_2\text{P}_8\text{W}_{48}\text{O}_{186}] \cdot 132\text{H}_2\text{O}$, is synthesized under relatively mild conditions, involving first the preparation of $\{P_8W_{48}\}$ building clusters and subsequently the reaction of these clusters with $\text{Co}(\text{ClO}_4)_2 \cdot 6\text{H}_2\text{O}$ in aqueous

media. The mechanism of this large, all-inorganic crystal-to-crystal transformation is attributed to the stability of the ring-shaped clusters and their ability to reorganize within the crystal lattice. This reorganization is facilitated by the facile forming and breaking of $\text{W}-\text{O}(\text{W})$ and $\text{Co}-\text{O}(\text{W})$ bonds between the linkers and inorganic rings in the crystal lattice.

Another approach for the preparation of all-inorganic framework materials is the use of non-coordinating (weakly complexing) ligands. In fact, Ag^+ dimers can be used as linking units in conjunction with larger isopolyoxometalates to construct 3D frameworks as long as only weakly coordinating ligands are used to ensure the Ag^+ ions coordinate the metal-oxo framework^{98,131} (FIG. 9). Here, infinite arrays of $\{W_{12}\}^{5-}$ α -metatungstic clusters are connected to eight $\{\text{Ag}_2\}^{2+}$ cations by coordination through the terminal $\text{W}=\text{O}$ oxygen bonds. The $\text{W}-\text{O}-\text{Ag}$ bridges provide flexibility and stability that enable the assembly of an infinite purely covalently connected inorganic framework. A driving force for the assembly of the framework is the formation of eight $\{\text{Ag}_2\}^{2+}$ dimers around the Keggin-type $\{W_{12}\}^{5-}$ anion, and the $\text{Ag}^+ \cdots \text{Ag}^+$ argentophilic metal-metal interactions are key for the stability of the 3D network of microporous channel assembly. The walls of the micropores are composed of a cage-like assembly of four $\{W_{12}\}^{5-}$ clusters and two $\{\text{Ag}_2\}^{2+}$ dimers, and the charge of the system is balanced by the presence of $[\text{Ag}(\text{CH}_3\text{CN})_4]^+$ in the ion channels. The material shows reversible sorption and desorption of small organic molecules, such as acetonitrile, and can undergo very interesting reductive chemistry⁹⁸.

The best way to engineer redox and electronically active frameworks is to incorporate POM clusters. For example, the so-called Keggin-Net is a family of extended modular 3D frameworks that are redox-active (FIG. 10). These are pure metal oxide frameworks based on substituted Keggin-type POM building blocks $[\{W_{72}M_{12}O_{268}X_7\}_n]^{y-}$, where $M = \text{Mn}^{\text{III/IV}}$ or $\text{Co}^{\text{III/IV}}$ and $X = \text{Si}^{\text{IV}}$ or Ge^{IV} . This framework is composed solely of cluster anions that are connected by symmetry equivalent $\text{W}-\text{O}-\text{M}$ linkages. Above those linkages, the W and the Co or Mn atoms are disordered over the $M_1-\text{O}-M_2$ unit such that $M_1 \neq M_2$ (that is, $\text{M}-\text{O}-\text{W}$ and $\text{W}-\text{O}-\text{M}$). The structure of this material is described as an infinite array of 3-connected and 4-connected Keggin polyanions. This material can undergo a reversible redox process that involves the simultaneous inclusion of the redox reagent with a concerted and spatially ordered redox change of the framework^{98,142-144}. The possibility of using this redox-active framework to monitor electron transfer reactions and catalysis by mixing Co and Mn in the POM is currently being explored. Also, the use of a redox-active framework to substitute different metal ions is interesting because it introduces the concept of a redox alloy⁹⁸: that is, numerous POM frameworks with differing fractions of redox-active metals — for example, Co , Ni and Mn — ‘doped’ into the framework. Despite the limitations of using only two main structural components (the cyclic POM $\{P_8W_{48}\}$ and a transition metal), there are already 14 unique POMzite-based framework materials based on this system¹⁴¹.

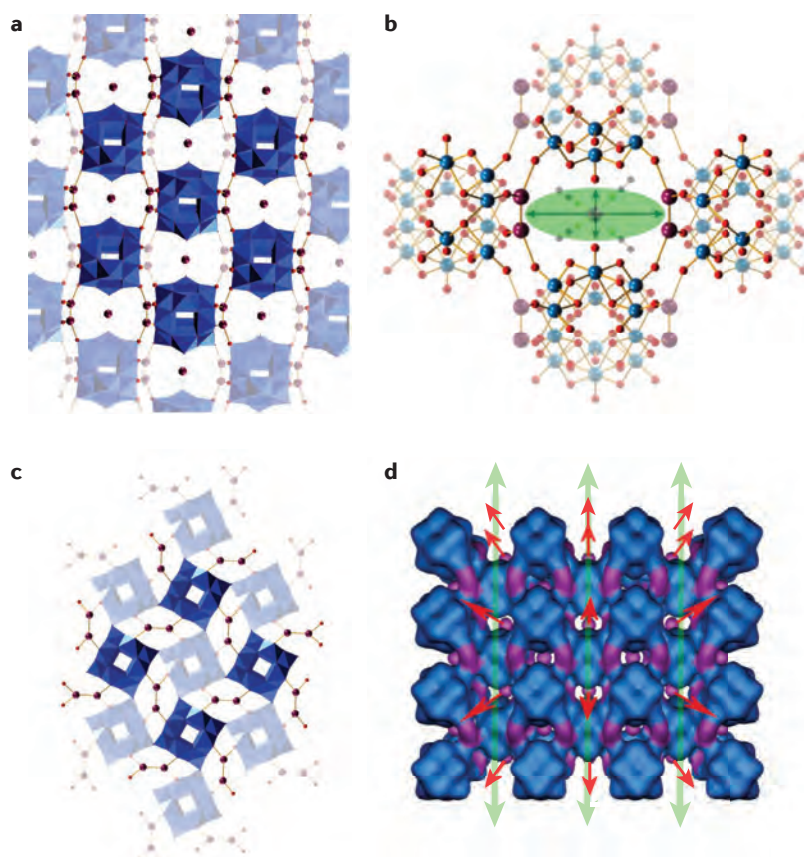


Figure 9 | Modular assembly of a 3D polyoxometalate open framework: $[\text{Ag}(\text{CH}_3\text{CN})_4]^+ \subset \{[\text{Ag}(\text{CH}_3\text{CN})_2]_4[\text{H}_5\text{W}_{12}\text{O}_{40}]\}$ with $\text{Ag}^+ \cdots \text{Ag}^+$ interactions. **a** | The $\{W_{12}\}^{5-}$ units (blue) and $\{\text{Ag}_2\}^{2+}$ dimers (purple) arrange to form channels in which the $[\text{Ag}(\text{CH}_3\text{CN})_4]^+$ counterions are located. **b** | A detailed illustration of the channels that shows the pore as a green ellipsoid. **c** | A different view of the framework showing the bridging mode of the $\{\text{Ag}_2\}^{2+}$ dimers. **d** | A space-filling representation of the framework indicating the propagation of the channels (red and green arrows). Solvent molecules are omitted for clarity. Figure is reproduced with permission from REF. 131, Wiley-VCH.

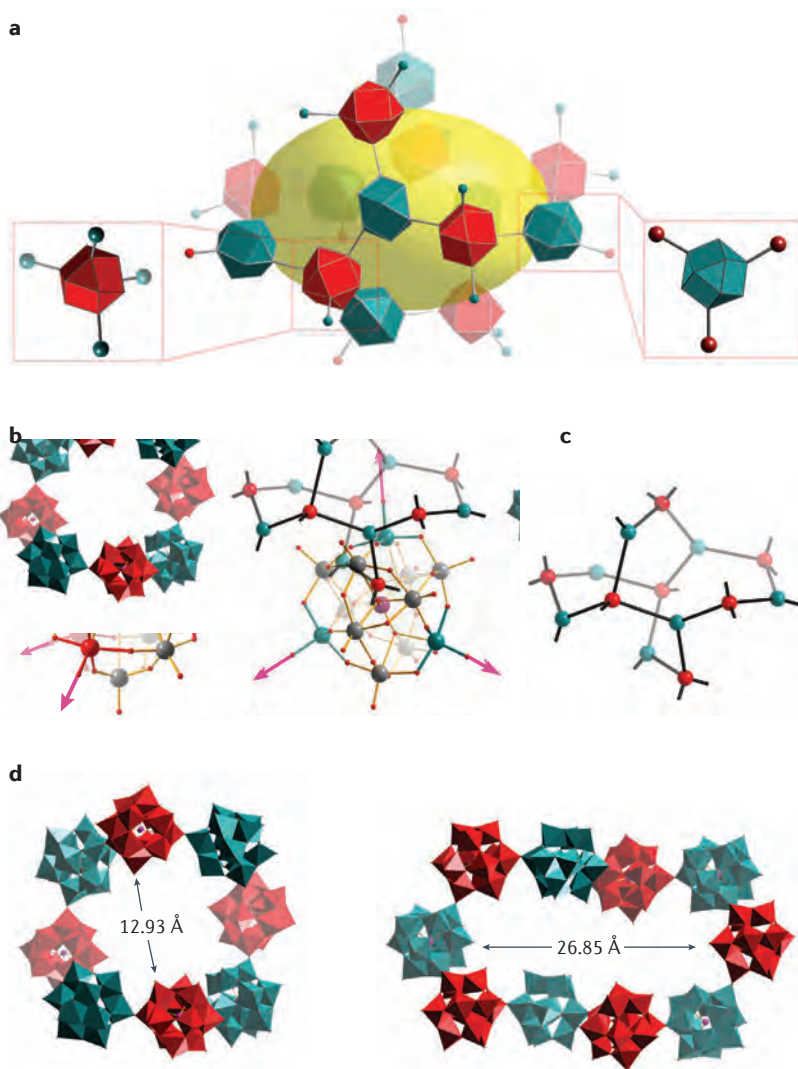


Figure 10 | Illustration of the nanosized pockets in a pure Keggin network. **a** | The pure Keggin network $\{[W_{12}M_{12}O_{268}X_n]_n\}^{n-}$, where $M = Mn^{IV}$ or Co^{III} and $X = Si^{IV}$ or Ge^{IV} . The pore (dimensions: $2.7 \times 2.4 \times 1.3$ nm) is highlighted by a yellow ellipsoid. The 3-connected and 4-connected Keggin clusters (green and red, respectively) show the connectivity of each unit. **b** | The right and left panels show the trigonal-connecting and tetrahedral-connecting building blocks. The arrows indicate the connecting modes. **c** | A view of the internal pocket of the Keggin network. **d** | Polyhedral representations of an 8-membered ring in the left panel and of a 10-membered ring in the right panel illustrating the smallest and largest dimensions of the pocket. Figure is reproduced with permission from REF. 98, Wiley-VCH.

Outlook

Many researchers endeavour to design new MOFs and to expand the variety of structures, tune surface areas, enhance properties and develop further applications. But why are MOFs so attractive? In part, their success is a consequence of the *ab initio* methods used to design structures combined with their facile synthesis (just mix a complex metal ion with a well-chosen ligand under solvothermal conditions and MOF crystals appear within hours). By contrast, although molecular metal oxides have well-known cluster structures, the formation of materials is, in general, more haphazard than for MOFs. However, this is slowly changing; we are

beginning to establish rules that may allow us to make frameworks with interesting topologies, symmetries and electronic redox properties. These rules hint towards a structural design revolution and show the potential to design and synthesize new POM-based materials. First, POMs with intrinsic integrated pores can be used as molecular panelling to make porous frameworks with pore sizes that are equivalent to those of the starting POM. This is in contrast to the pores of MOFs that are designed but arise from the assembly of the components and are hence extrinsic. Second, POMs decorated with ligands undergo the same topological design principles as MOFs. Third, the coordination of the exo-oxygen of POMs with first-row transition metals has the ability to produce a large range of structures. The reaction conditions control the topology and structure of the resultant material, which is both a source of frustration and discovery.

In the near future, it may be possible to produce catalytically active or multifunctional materials that have several roles encoded into a single material. For example, the combination of a cluster capable of redox activity, a cluster capable of small-molecule binding and a cluster capable of photochemical activation could produce a material with all of these characteristics. The challenge is selecting the optimal POM and metal-ion linker, as well as engineering their assembly in an efficient and high-yielding manner.

Despite our optimism, we are still far from being able to apply the same principles used in the assembly of MOFs to form linkable POM clusters. To advance this area, we need to combine design and computational modelling to imagine a wide range of different rearrangements and to create a blueprint for building these materials¹⁴⁵. Also, the preparation of POM-OFs and POMzites has been limited by the sensitive nature of the synthesis of many POMs. However, our knowledge of self-assembly and system automation is advancing such that the preparation of these building blocks is becoming much easier. Another synthetic challenge to overcome is to ensure that the porous structures are stable, in particular, in the presence of water. Attaining this stability requires the correct linkers to be used to ensure that the structures do not dissolve too quickly. Finally, the structural determination of the POM-based frameworks must be speeded up to prevent this from becoming a bottleneck in the process. Adaption of crystallographic methods used to determine protein structures, as well as non-crystallographic tools, such as cryo-electron tomography, are likely techniques to achieve this.

With improving synthetic access and characterization, combined with libraries of new building blocks and the proposed way of classifying the resultant structures¹⁴¹, POM-based frameworks are emerging as a class of metal oxide materials. In particular, we believe that the development of POMzites may enter a new era. The result will be that the familiar and technologically vital metal oxides, designed using topological bottom-up approaches to form large-panelled structures, will enter the realm of the MOF age.

- Philp, D. & Stoddart, J. F. Self-assembly in natural and unnatural systems. *Angew. Chem. Int. Ed. Engl.* **35**, 1154–1196 (1996).
- Whitesides, G. M. & Grzybowski, B. Self-assembly at all scales. *Science* **295**, 2418–2421 (2002).
- Koblenz, T. S., Wassenaar, J. & Reek, J. N. H. Reactivity within a confined self-assembled nanospace. *Chem. Soc. Rev.* **37**, 247–262 (2008).
- Kresge, C. T., Leonowicz, M. E., Roth, W. J., Vartuli, J. C. & Beck, J. S. Ordered mesoporous molecular sieves synthesized by a liquid-crystal template mechanism. *Nature* **539**, 710–712 (1992).
- Li, H., Eddaoudi, M., O’Keeffe, M. & Yaghi, O. M. Design and synthesis of an exceptionally stable and highly porous metal–organic framework. *Nature* **402**, 276–279 (1999).
- Eddaoudi, M. *et al.* Systematic design of pore size and functionality in isorecticular MOFs and their application in methane storage. *Science* **295**, 469–472 (2002).
- Wang, B., Côté, A. P., Furukawa, H., O’Keeffe, M. & Yaghi, O. M. Colossal cages in zeolitic imidazolate frameworks as selective carbon dioxide reservoirs. *Nature* **453**, 207–212 (2008).
- Morris, R. E. & Wheatley, P. S. Gas storage in nanoporous materials. *Angew. Chem. Int. Ed.* **47**, 4966–4981 (2008).
- Li, J.-R., Kuppler, R. J. Y. & Zhou, H.-C. Selective gas adsorption and separation in metal–organic frameworks. *Chem. Soc. Rev.* **38**, 1477–1504 (2009).
- James, S. L. Metal–organic frameworks. *Chem. Soc. Rev.* **32**, 276–288 (2003).
- Mann, S. & Ozin, G. A. Synthesis of inorganic materials with complex form. *Nature* **382**, 313–318 (1996).
- Barrer, R. M. *Zeolites and Clay Minerals as Sorbents and Molecular Sieves* Ch. 1.2.6 (Academic, 1978).
- Cundy, C. S. & Cox, P. A. The hydrothermal synthesis of zeolites: history and from the earliest days to the present time. *Chem. Rev.* **103**, 663–701 (2003).
- Mumpton, F. A. *La roca magica: uses of natural zeolites in agriculture and industry. Proc. Natl Acad. Sci. USA* **96**, 3463–3470 (1999).
- Moliner, M., Martínez, C. & Corma, A. Multipore zeolites: synthesis and catalytic applications. *Angew. Chem. Int. Ed.* **54**, 3560–3579 (2015).
- Davis, M. E. & Lobo, R. F. Zeolite and molecular sieve synthesis. *Chem. Mater.* **4**, 756–768 (1992).
- Barrer, R. M. Syntheses and reactions of mordenite. *J. Chem. Soc.* **127**, 2158–2163 (1948).
- Kokotailo, G., Lawton, S. & Olson, D. Structure of synthetic zeolite ZSM 5. *Nature* **272**, 437–438 (1978).
- Davis, M. E. Ordered porous materials for emerging applications. *Nature* **417**, 813–821 (2002).
- Valtchev, V., Majano, G., Mintova, S. & Pérez-Ramírez, J. Tailored crystalline microporous materials by post-synthesis modification. *Chem. Soc. Rev.* **42**, 263–290 (2013).
- Wilson, S. T., Lok, B. M., Messina, C. A., Cannon, T. R. & Flanigen, E. M. Aluminophosphate molecular sieves: a new class of microporous crystalline inorganic solids. *J. Am. Chem. Soc.* **104**, 1146–1147 (1982).
- Harvey, G. & Meier, W. M. The synthesis of beryllophosphate zeolites. *Stud. Surf. Sci. Catal.* **A49**, 411–420 (1989).
- Gier, T. E. & Stucky, G. D. Low-temperature synthesis of hydrated zinc(beryllo)-phosphate and arsenate molecular sieves. *Nature* **349**, 508–510 (1991).
- Gier, T. E., Bu, X. H., Feng, P. Y. & Stucky, G. D. Synthesis and organization of zeolite-like materials with three-dimensional helical pores. *Nature* **395**, 154–157 (1998).
- Estermann, M., McCusker, L. B., Baerlocher, C., Merrouche, A. & Kessler, H. A synthetic gallophosphate molecular sieve with a 20 tetrahedral-atom pore opening. *Nature* **352**, 320–323 (1991).
- Davis, M. E. Grand openings for cloverite. *Nature* **352**, 281–282 (1991).
- Wright, P. A., Morris, R. E. & Wheatley, P. S. Synthesis of microporous materials using macrocycles as structure directing agents. *Dalton Trans.* 5359–5368 (2007).
- Jiang, J. *et al.* Synthesis and structure determination of the hierarchical mesomicroporous zeolite ITQ 43. *Science* **333**, 1131–1134 (2011).
- Lewis, D. W., Willock, D. J., Catlow, C. R. A., Thomas, J. M. & Hutchings, G. J. *De novo* design of structure-directing agents for the synthesis of microporous solids. *Nature* **382**, 604–606 (1996).
- Simancas, R. *et al.* Modular organic structure-directing agents for the synthesis of zeolites. *Science* **330**, 1219–1222 (2010).
- Sun, J. *et al.* The ITQ 37 mesoporous chiral zeolite. *Nature* **458**, 1154–1157 (2009).
- Tang, L. *et al.* A zeolite family with chiral and achiral structures built from the same building layer. *Nat. Mater.* **7**, 381–385 (2008).
- Baerlocher, C. *et al.* Ordered silicon vacancies in the framework structure of the zeolite catalyst SSZ 74. *Nat. Mater.* **7**, 631–635 (2008).
- Baerlocher, C. *et al.* Structure of the polycrystalline zeolite catalyst IM 5 solved by enhanced charge flipping. *Science* **315**, 1113–1116 (2007).
- Roth, W. J. *et al.* A family of zeolites with controlled pore size prepared using a top-down method. *Nat. Chem.* **5**, 628–633 (2013).
- Furukawa, H. *et al.* The chemistry and applications of metal–organic frameworks. *Science* **341**, 1230444 (2013).
- Férey, G. Hybrid porous solids: past, present, future. *Chem. Soc. Rev.* **37**, 191–214 (2008).
- Cavka, J. H. *et al.* A new zirconium inorganic building brick forming metal organic frameworks with exceptional stability. *J. Am. Chem. Soc.* **130**, 13850–13851 (2008).
- Marshall, R. J. & Forgan, R. S. Postsynthetic modification of zirconium metal–organic frameworks. *Eur. J. Inorg. Chem.* **27**, 4310–4331 (2016).
- Rodríguez-Albelo, L. M. *et al.* Zeolitic polyoxometalate-based metal-organic frameworks (Z-POMOFs): computational evaluation of hypothetical polymorphs and the successful targeted synthesis of the redox-active Z-POMOF1. *J. Am. Chem. Soc.* **131**, 16078–16087 (2009).
- Miras, H. N., Vilà-Nadal, L. & Cronin, L. Polyoxometalate based open-frameworks (POM-OFs). *Chem. Soc. Rev.* **43**, 5679–5699 (2014).
- Pope, M. T. & Müller, A. (eds) *Polyoxometalates: from Platonic Solids to Anti-Retroviral Activity* (Kluwer Academic Publishers, 1994).
- Proust, A. *et al.* Functionalization and post-functionalization: a step towards polyoxometalate-based materials. *Chem. Soc. Rev.* **41**, 7605–7622 (2012).
- Song, Y.-F. & Tsunashima, R. Recent advances on polyoxometalate-based molecular and composite materials. *Chem. Soc. Rev.* **41**, 7384–7402 (2012).
- Miras, H. N., Yan, J., Long, D.-L. & Cronin, L. Engineering polyoxometalates with emergent properties. *Chem. Soc. Rev.* **41**, 7403–7430 (2012).
- Long, D.-L., Burkholder, E. & Cronin, L. Polyoxometalate clusters, nanostructures and materials: from self assembly to designer materials and devices. *Chem. Soc. Rev.* **36**, 105–121 (2007).
- Hill, C. L. & Prosser-McCarthy, C. M. Homogeneous catalysis by transition oxygen anion clusters. *Coord. Chem. Rev.* **143**, 407–455 (1995).
- Dolbecq, A., Dumas, E., Cédric, R. M. & Mialane, P. Hybrid organic–inorganic polyoxometalate compounds: from structural diversity to applications. *Chem. Rev.* **110**, 6009–6048 (2010).
- Binnemans, K. Lanthanide-based luminescent hybrid materials. *Chem. Rev.* **109**, 4233–4374 (2009).
- Ormwoma, S., Chen, W., Tsunashima, R. & Song, Y.-F. Recent advances on polyoxometalates intercalated layered double hydroxides: from synthetic approaches to functional material applications. *Coord. Chem. Rev.* **258**, 58–71 (2014).
- Nyman, M. & Burns, P. C. A comprehensive comparison of transition-metal and actinyl polyoxometalates. *Chem. Soc. Rev.* **41**, 7354–7367 (2012).
- Clemente-Juan, J. M., Coronado, E. & Gaita-Ariño, A. Magnetic polyoxometalates: from molecular magnetism to molecular spintronics and quantum computing. *Chem. Soc. Rev.* **41**, 7464–7478 (2012).
- Polarz, S., Landsmann, S. & Kläiber, A. Hybrid surfactant systems with inorganic constituents. *Angew. Chem. Int. Ed.* **53**, 946–954 (2014).
- Kitagawa, S., Kitaura, R. & Noro, S. Functional porous coordination polymers. *Angew. Chem. Int. Ed.* **43**, 2334–2375 (2004).
- Sumida, K. *et al.* Carbon dioxide capture in metal–organic frameworks. *Chem. Rev.* **112**, 724–781 (2012).
- Luger, K., Mader, A. W., Richmond, R. K., Sargent, D. F. & Richmond, T. J. Crystal structure of the nucleosome core particle at 2.8 Å resolution. *Nature* **389**, 251–260 (1997).
- Krivovichev, S. V. Which inorganic structures are the most complex? *Angew. Chem. Int. Ed.* **53**, 654–661 (2014).
- Liu, T., Diemann, E., Li, H., Dress, A. W. M. & Müller, A. Self-assembly in aqueous solution of wheel-shaped Mo154 oxide clusters into vesicles. *Nature* **426**, 59–62 (2003).
- Mitra, T. *et al.* Gated and differently functionalized (new) porous capsules direct encapsulates’ structures: higher and lower density water. *Chem. Eur. J.* **15**, 1844–1852 (2009).
- Müller, A., Beckmann, E., Bögge, H., Schmidtman, M. & Dress, A. Inorganic chemistry goes protein size: a Mo₃₆₈ nano-hedgehog initiating nanochemistry by symmetry breaking. *Angew. Chem. Int. Ed.* **41**, 1162–1167 (2002).
- Weber, T. *et al.* Large, larger, largest — a family of cluster-based tantalum copper aluminides with giant unit cells. I. Structure solution and refinement. *Acta Cryst.* **B65**, 308–317 (2009).
- Lister, S. E., Evans, I. R. & Evans, J. S. O. Complex superstructures of Mo₂P₂O₁₅. *Inorg. Chem.* **48**, 9271–9281 (2009).
- Lindqvist, I. On the structure of the paratungstate ion. *Acta Cryst.* **5**, 667–670 (1952).
- Keggin, F. J. Structure of the molecule of 12 phosphotungstic acid. *Nature* **131**, 908–909 (1933).
- Dawson, B. The structure of the 9(18)-heteropoly anion in potassium 9(18)-tungstophosphate, K₉(P₂W₁₈O₆₂·14H₂O). *Acta Cryst.* **6**, 113–126 (1953).
- Alizadeh, M. H., Harmalkar, S. P., Jeannin, Y., Martin-Frère, J. & Pope, M. T. A heteropolyanion with fivefold molecular symmetry that contains a nonlabile encapsulated sodium ion. The structure and chemistry of [NaP₂W₁₈O₆₂]¹⁴⁻. *J. Am. Chem. Soc.* **107**, 2662–2669 (1985).
- Rong, C. & Pope, M. T. Lacunary polyoxometalate anions are π acceptor ligands. Characterization of some tungstotriphenate(μ₃, μ₂, μ) heteropolyanions and their atom-transfer reactivity. *J. Am. Chem. Soc.* **114**, 2932–2938 (1992).
- Black, J. R., Nyman, M. & Casey, W. H. Rates of oxygen exchange between the [H₂Nb₂O₁₀]⁸⁻ (aq) Lindqvist ion and aqueous solutions. *J. Am. Chem. Soc.* **128**, 14712–14720 (2006).
- Sloan, J. *et al.* Direct imaging of the structure, relaxation, and sterically constrained motion of encapsulated tungsten polyoxometalate Lindqvist ions within carbon nanotubes. *ACS Nano* **2**, 966–976 (2008).
- Vilà-Nadal, L. *et al.* Combined theoretical and mass spectrometry study of the formation-fragmentation of small polyoxomolybdates. *Inorg. Chem.* **50**, 7811–7819 (2011).
- Vilà-Nadal, L. *et al.* Nucleation mechanisms of molecular oxides: a study of the assembly-disassembly of [W₆O₁₃]²⁻ by theory and mass spectrometry. *Angew. Chem. Int. Ed.* **48**, 5452–5456 (2009).
- Vilà-Nadal, L., Rodríguez-Fortea, A. & Poblet, J. M. Theoretical analysis of the possible intermediates in the formation of [W₆O₁₃]²⁻. *Eur. J. Inorg. Chem.* 5125–5133 (2009).
- Long, D.-L., Kögerler, P., Parenty, A. D. C., Fielden, J. & Cronin, L. Discovery of a family of isopolyoxotungstates [H₂W₁₀O₃₂]⁶⁻ encapsulating a {WO₆} moiety within a {W₁₈} Dawson-like cluster cage. *Angew. Chem. Int. Ed.* **45**, 4798–4803 (2006).
- Vilà-Nadal, L. *et al.* Polyoxometalate {W₁₈O₆₆XO₆} clusters with embedded redox-active main-group templates as localized inner-cluster radicals. *Angew. Chem. Int. Ed.* **52**, 9695–9699 (2013).
- Busche, C. *et al.* Design and fabrication of memory devices based on nanoscale polyoxometalate clusters. *Nature* **515**, 545–549 (2014).
- Müller, A. & Gouzerh, P. From linking of metal-oxide building blocks in a dynamic library to giant clusters with unique properties and towards adaptive chemistry. *Chem. Soc. Rev.* **41**, 7431–7463 (2012).
- Pradeep, C. P., Long, D.-L. & Cronin, L. Cations in control: crystal engineering polyoxometalate clusters using cation directed self-assembly. *Dalton Trans.* **39**, 9443–9457 (2010).
- Cheong, S. W. Transition metal oxides: the exciting world of orbitals. *Nat. Mater.* **6**, 927–928 (2007).
- Bassil, B. S. & Körtz, U. Divacant polyoxotungstates: reactivity of the gamma-decatungstates [γ-XW₁₀O₃₅]⁸⁻ (X = Si, Ge). *Dalton Trans.* **40**, 9649 (2011).
- Zhang, Z. *et al.* Two multi-copper-containing heteropolyoxotungstates constructed from the lacunary Keggin polyoxoanion and the high-nuclear spin cluster. *Inorg. Chem.* **46**, 8162–8169 (2007).
- Winter, R. S., Long, D.-L. & Cronin, L. Synthesis and characterization of a series of [M₂(β-SiW₈O₃₁)₂]⁸⁻ clusters and mechanistic insight into the reorganization of {β-SiW₈O₃₁} into {α-SiW₈O₃₄}. *Inorg. Chem.* **54**, 4151–4155 (2015).

82. Zhang, Z. *et al.* Synthesis, characterization, and crystal structures of two novel high-nuclear nickel-substituted dimeric polyoxometalates. *Inorg. Chem.* **45**, 4313–4315 (2006).
83. Assran, A. S. *et al.* Alpha and beta isomers of tetrafluorine(IV) containing decatungstosilicates, $[\text{Hf}(\text{OH})_6(\text{CH}_3\text{COO})_2(x\text{-SiW}_9\text{O}_{37})]^{12-}$ ($x = \alpha, \beta$). *Dalton Trans.* **40**, 2920–2925 (2011).
84. Bassil, B. S. *et al.* A planar $\{\text{Mn}_{10}(\text{OH})_{12}\}^{26+}$ unit incorporated in a 60 tungsto-6 silicate polyanion. *Angew. Chem. Int. Ed.* **50**, 5961–5964 (2011).
85. Winter, R. S. *et al.* Nanoscale control of polyoxometalate assembly: a $\{\text{Mn}_8\text{W}_4\}$ cluster within a $\{\text{W}_{36}\text{Si}_4\text{Mn}_{10}\}$ cluster showing a new type of isomerism. *Chem. Eur. J.* **19**, 2976–2981 (2013).
86. Hussain, F., Bassil, B. S., Bi, L. H., Reicke, M. & Körtz, U. Structural control on the nanomolecular scale: self-assembly of the polyoxotungstate wheel $[\{\beta = \text{Ti}_2\text{SiW}_{10}\text{O}_{38}\}_n]^{24-}$. *Angew. Chem. Int. Ed.* **43**, 3485–3488 (2004).
87. Mitchell, S. G. *et al.* A mixed-valence manganese cubane trapped by inequivalent trilacunary polyoxometalate ligands. *Angew. Chem. Int. Ed.* **50**, 9154–9157 (2011).
88. Zheng, S. T., Zhang, J., Clemente-Juan, J. M., Yuan, D. Q. & Yang, G. Poly(polyoxotungstate)s with 20 nickel centers: from nanoclusters to one-dimensional chains. *Angew. Chem. Int. Ed.* **48**, 7176–7179 (2009).
89. Huang, L., Wang, S.-S., Zhao, J.-W., Cheng, L. & Yang, G.-Y. Synergistic combination of multi-Zr^{IV} cations and lacunary Keggin germanotungstates leading to a gigantic Zr₂₄-cluster-substituted polyoxometalate. *J. Am. Chem. Soc.* **136**, 7637–7642 (2014).
90. Sartorel, A. *et al.* Polyoxometalate embedding of a tetrathurium(IV)-oxo-core by template-directed metalation of $[\gamma\text{-SiW}_9\text{O}_{36}]^{8-}$: a totally inorganic oxygen-evolving catalyst. *J. Am. Chem. Soc.* **130**, 5006–5007 (2008).
91. Stracke, J. J. & Finke, R. G. Distinguishing homogeneous from heterogeneous water oxidation catalysis when beginning with polyoxometalates. *ACS Catal.* **4**, 909–935 (2014).
92. Kamata, K. *et al.* Efficient epoxidation of olefins with $\geq 99\%$ selectivity and use of hydrogen peroxide. *Science* **300**, 964–966 (2003).
93. Ritchie, C. *et al.* Polyoxometalate-mediated self-assembly of single-molecule magnets: $\{[\text{XW}_9\text{O}_{36}]_n[\text{Mn}^{\text{II}}, \text{Mn}^{\text{III}}\text{O}_4(\text{H}_2\text{O})_4]^{12-}\}$. *Angew. Chem. Int. Ed.* **47**, 5609–5612 (2008).
94. Ge, M., Zhong, B., Klemperer, W. G. & Gewirth, A. A. Self-assembly of silicotungstate anions on silver surfaces. *J. Am. Chem. Soc.* **118**, 5812–5813 (1996).
95. Klonowski, P. *et al.* Synthesis and characterization of the platinum-substituted Keggin anion $\alpha\text{-H}_2\text{SiPtW}_{11}\text{O}_{40}^{4-}$. *Inorg. Chem.* **53**, 13239–13246 (2014).
96. Cameron, J. M. *et al.* Investigating the transformations of polyoxoanions using mass spectrometry and molecular dynamics. *J. Am. Chem. Soc.* **138**, 8765–8773 (2016).
97. Saalfrank, R. W., Maid, H. & Scheurer, A. Supramolecular coordination chemistry: the synergistic effect of serendipity and rational design. *Angew. Chem. Int. Ed.* **47**, 8795–8824 (2008).
98. Ritchie, C. *et al.* Reversible redox reactions in an extended polyoxometalate framework solid. *Angew. Chem. Int. Ed.* **47**, 6881–6884 (2008).
99. Khenkin, A. M., Weiner, L., Wang, Y. & Neumann, R. Electron and oxygen transfer in polyoxometalate, $\text{H}_2\text{PV}_2\text{Mo}_{10}\text{O}_{40}$, catalyzed oxidation of aromatic and alkyl aromatic compounds: evidence for aerobic Mars-van Krevelen-type reactions in the liquid homogeneous phase. *J. Am. Chem. Soc.* **123**, 8531–8542 (2001).
100. Kastner, K. *et al.* Controlled reactivity tuning of metal-functionalized vanadium oxide clusters. *Chem. Eur. J.* **21**, 7686–7689 (2015).
101. Martin-Sabi, M. *et al.* Rearrangement of $\{\alpha\text{-P}_2\text{W}_{15}\}$ to $\{\text{PW}_6\}$ moieties during the assembly of transition-metal-linked polyoxometalate clusters. *Chem. Commun.* **52**, 919–921 (2016).
102. Zheng, Q. *et al.* Following the reaction of heteroanions inside a $\{\text{W}_{18}\text{O}_{54}\}$ polyoxometalate nanocage by NMR spectroscopy and mass spectrometry. *Angew. Chem. Int. Ed.* **54**, 7895–7899 (2015).
103. Macdonell, A., Johnson, N. B., Surman, A. J. & Cronin, L. Configurable nonoxidative metal oxide oligomers via precise ‘click’ coupling control of hybrid polyoxometalates. *J. Am. Chem. Soc.* **137**, 5662–5665 (2015).
104. Sadeghi, O., Zakharov, L. N. & Nyman, M. Crystal growth. Aqueous formation and manipulation of the iron-oxo Keggin ion. *Science* **347**, 1359–1362 (2015).
105. Winter, R. S., Cameron, J. M. & Cronin, L. Controlling the minimal self assembly of complex polyoxometalate clusters. *J. Am. Chem. Soc.* **136**, 12753–12761 (2014).
106. Long, D.-L. *et al.* Capture of periodate in a $\{\text{W}_{18}\text{O}_{54}\}$ cluster cage yielding a catalytically active polyoxometalate $[\text{H}_2\text{W}_{18}\text{O}_{56}(\text{IO}_4)]^{6-}$ embedded with high-valent iodine. *Angew. Chem. Int. Ed.* **47**, 4384–4387 (2008).
107. Yan, J., Long, D.-L., Wilson, E. F. & Cronin, L. Discovery of heteroatom-embedded $\text{Te}^{\text{IV}}\{\text{W}_{18}\text{O}_{54}\}$ nanofunctional polyoxometalates by use of cryospray mass spectrometry. *Angew. Chem. Int. Ed.* **48**, 4376–4380 (2009).
108. Ritchie, C. *et al.* Exploiting the multifunctionality of organocations in the assembly of hybrid polyoxometalate clusters and networks. *Chem. Commun.* **5**, 468–470 (2007).
109. Cameron, J. M., Gao, J., Vilà-Nadal, L., Long, D.-L. & Cronin, L. Formation, self-assembly and transformation of a transient selenotungstate building block into clusters, chains and macrocycles. *Chem. Commun.* **50**, 2155–2157 (2014).
110. Mizuno, N. & Uchida, S. Structures and sorption properties of ionic crystals of polyoxometalates with macrocage. *Chem. Lett.* **35**, 688–693 (2006).
111. Kawamoto, R., Uchida, S. & Mizuno, N. Amphiphilic guest sorption of $\text{K}_3[\text{Cr}_3(\text{O}(\text{OOC})_2\text{H}_5)_6(\text{H}_2\text{O})_2][\alpha\text{-SiW}_9\text{O}_{36}]$ ionic crystal. *J. Am. Chem. Soc.* **127**, 10560–10567 (2005).
112. Okamoto, K., Uchida, S., Ito, T. & Mizuno, N. Self-organization of all-inorganic dodecatungstophosphate nanocrystallites. *J. Am. Chem. Soc.* **129**, 7378–7384 (2007).
113. Suzuki, K. *et al.* Three-dimensional ordered arrays of $58 \times 58 \times 58 \text{ \AA}^3$ hollow frameworks in ionic crystals of M_2Zn_2 -substituted polyoxometalates. *Angew. Chem. Int. Ed.* **51**, 1597–1601 (2012).
114. Khan, M. I., Yohannes, E. & Doedens, R. $[\text{M}_2\text{V}_{18}\text{O}_{54}(\text{H}_2\text{O})_2(\text{XO})_2] \cdot 24\text{H}_2\text{O}$ ($\text{M} = \text{Fe}, \text{Co}; \text{X} = \text{V}, \text{S}$): metal oxide based framework materials composed of polyoxovanadate clusters. *Angew. Chem. Int. Ed.* **38**, 1292–1294 (1999).
115. Wang, X.-L. *et al.* Polyoxometalate-based porous framework with perovskite topology. *Crys. Growth Des.* **10**, 4227–4230 (2010).
116. Takashima, Y., Miras, H. N., Glatzel, S. & Cronin, L. Shrink wrapping redox-active crystals of polyoxometalate open frameworks with organic polymers via crystal induced polymerisation. *Chem. Commun.* **52**, 7794–7797 (2016).
117. Yue, L. *et al.* Flexible single-layer ionic organic-inorganic frameworks toward precise nano-size separation. *Nat. Commun.* **7**, 10742 (2016).
118. Ma, H. *et al.* Cationic covalent organic frameworks: a simple platform of anionic exchange porosity tuning and proton conduction. *J. Am. Chem. Soc.* **138**, 5897–5903 (2016).
119. Qin, J. S. *et al.* Ultraporous polymolybdate-based metal-organic frameworks as highly active electrocatalysts for hydrogen generation from water. *J. Am. Chem. Soc.* **137**, 7169–7177 (2015).
120. Shi, D. *et al.* A photosensitized decatungstate-based MOF as heterogeneous photocatalyst for the selective C–H alkylation of aliphatic nitriles. *Chem. Commun.* **52**, 4714–4717 (2016).
121. Salomon, W. *et al.* Immobilization of polyoxometalates in the Zr based metal organic framework UiO-67. *Chem. Commun.* **51**, 2972–2975 (2015).
122. Lysenko, A. B. *et al.* Synthesis and structural elucidation of triazolyimolybdenum(IV) oxide hybrids and their behavior as oxidation catalysts. *Inorg. Chem.* **54**, 8327–8338 (2015).
123. Watfa, N. *et al.* Two compartmentalized inner receptors for the tetramethylammonium guest within a keplerate-type capsule. *Inorg. Chem.* **55**, 9368–9376 (2016).
124. Sadeghi, O. *et al.* Chemical stabilization and electrochemical destabilization of the iron Keggin ion in water. *Inorg. Chem.* **55**, 11078–11088 (2016).
125. Guo, L. Y. *et al.* A pyridazine-bridged sandwiched cluster incorporating planar hexanuclear cobalt ring and bivalent phosphotungstate. *Inorg. Chem.* **55**, 9006–9011 (2016).
126. Zhu, S. L. *et al.* Assembly of a metalloporphyrin-polyoxometalate hybrid material for highly efficient activation of molecular oxygen. *Inorg. Chem.* **55**, 7295–7300 (2016).
127. Martín-Caballero, J. *et al.* A robust open framework formed by decavanadate clusters and copper(II) complexes of macrocyclic polyamines: permanent microporosity and catalytic oxidation of cycloalkanes. *Inorg. Chem.* **55**, 4970–4979 (2016).
128. Li, H., Swenson, L., Doedens, R. J. & Khan, M. I. An organo-functionalized metal-oxide cluster, $[\text{V}_6\text{O}_6\{\text{O}(\text{CH}_2\text{CH}_2)_2\text{N}(\text{CH}_2\text{CH}_2\text{OH})_2\}]_n$, with Anderson-like structure. *Dalton Trans.* **45**, 16511–16518 (2016).
129. Mitchell, S. G., Boyd, T., Miras, H. N., Long, D.-L. & Cronin, L. Extended polyoxometalate framework solids: two Mn(II)-linked $\{\text{P}_8\text{W}_{48}\}$ network arrays. *Inorg. Chem.* **50**, 136–143 (2011).
130. Chen, S. W., Boubekeur, K., Gouzerh, P. & Proust, A. Versatile host-guest chemistry and networking ability of the cyclic tungstophosphate $\{\text{P}_8\text{W}_{48}\}$: two further manganese derivatives. *J. Mol. Struct.* **994**, 104–108 (2011).
131. Streb, C., Ritchie, C., Long, D.-L., Kögerler, P. & Cronin, L. Modular assembly of a functional polyoxometalate-based open framework constructed from unsupported Ag–Ag interactions. *Angew. Chem. Int. Ed.* **46**, 7579–7582 (2007).
132. Wang, X. L., Hu, H. L. & Tian, A. X. Influence of transition metal coordination nature on the assembly of multinuclear subunits in polyoxometalates-based compounds. *Cryst. Growth Des.* **10**, 4786–4794 (2010).
133. Wang, Y. *et al.* Hydrothermal syntheses and characterizations of two novel frameworks constructed from polyoxometalates, metals and organic units. *Dalton. Trans.* **39**, 1916–1919 (2010).
134. Mitchell, S. G. *et al.* Face-directed self-assembly of an electronically active Archimedean polyoxometalate architecture. *Nat. Chem.* **2**, 308–312 (2010).
135. Férey, G. *et al.* A chromium terephthalate-based solid with unusually large pore volumes and surface area. *Science* **309**, 2040–2042 (2005).
136. Liu, S. *et al.* Sodalite-type porous metal-organic framework with polyoxometalate templates: adsorption and decomposition of dimethyl methylphosphonate. *J. Am. Chem. Soc.* **133**, 4178–4181 (2011).
137. Song, J. *et al.* A multiunit catalyst with synergistic stability and reactivity: a polyoxometalate-metal organic framework for aerobic decontamination. *J. Am. Chem. Soc.* **133**, 16839–16846 (2011).
138. Contant, R. & Tézé, A. A new crown heteropolyanion $\text{K}_2\text{Li}_2\text{H}_2\text{P}_8\text{W}_{48}\text{O}_{184} \cdot 92\text{H}_2\text{O}$: synthesis, structure, and properties. *Inorg. Chem.* **24**, 4610–4614 (1985).
139. Sing, K. S. W. *et al.* Reporting physisorption data for gas/solid systems with special reference to the determination of surface area and porosity. *Pure Appl. Chem.* **54**, 603–619 (1985).
140. Zhan, C. *et al.* A metamorphic inorganic framework that can be switched between eight single-crystalline states. *Nat. Commun.* **8**, 14185 (2017).
141. Boyd, T. *et al.* POMzites: a family of zeolitic polyoxometalate frameworks from a minimal building block library. *J. Am. Chem. Soc.* **139**, 5930–5938 (2017).
142. Thiel, J., Ritchie, C., Streb, C., Long, D. L. & Cronin, L. Heteroatom-controlled kinetics of switchable polyoxometalate frameworks. *J. Am. Chem. Soc.* **131**, 4180–4181 (2009).
143. Thiel, J. *et al.* Modular inorganic polyoxometalate frameworks showing emergent properties: redox alloys. *Angew. Chem. Int. Ed.* **49**, 6984–6988 (2010).
144. Ritchie, C. *et al.* Spontaneous assembly and real-time growth of micrometre-scale tubular structures from polyoxometalate-based inorganic solids. *Nat. Chem.* **1**, 47–52 (2009).
145. Overvelde, J. T. B., Weaver, J. C., Hoberman, C. & Bertoldi, K. Rational design of reconfigurable prismatic architected materials. *Nature* **541**, 347–352 (2017).
146. Nazarian, D., Camp, J. S., Chung, Y. G., Snurr, R. Q. & Sholl, D. S. Large-scale refinement of metal-organic framework structures using density functional theory. *Chem. Mater.* **29**, 2521–2528 (2017).

147. Vilà-Nadal, L. Exploring the rotational isomerism in non-classical Wells–Dawson anions $\{W_{18}X\}$: a combined theoretical and mass spectrometry study. *Dalton Trans.* **41**, 2264–2271 (2012).
148. Mitchell, S. G. *et al.* Controlling nucleation of the cyclic heteropolyanion $\{P_8W_{48}\}$: a cobalt-substituted phosphotungstate chain and network. *Cryst. Eng. Commun.* **11**, 36–39 (2009).
149. Bassil, B. S. *et al.* Cobalt, manganese, nickel, and vanadium derivatives of the cyclic 48 tungsto-8 phosphate $[H_8P_8W_{48}O_{184}]^{35-}$. *Inorg. Chem.* **49**, 4949–4959 (2010).
150. Zhang, L. C. *et al.* Two new $\{P_8W_{49}\}$ wheel-shaped tungstophosphates decorated by Co(II), Ni(II) ions. *J. Cluster Sci.* **21**, 679–689 (2010).
151. Mitchell, S. G. *et al.* Extended polyoxometalate framework solids: two Mn(II)-linked $\{P_8W_{48}\}$ network arrays. *Inorg. Chem.* **50**, 136–143 (2011).
152. Chen, S.-W., Boubekeur, K., Gouzerh, P. & Proust, A. Versatile host–guest chemistry and networking ability of the cyclic tungstophosphate $\{P_8W_{48}\}$: two further manganese derivatives. *J. Mol. Struct.* **994**, 104–108 (2011).

Acknowledgements

L.V.-N. and L.C. gratefully acknowledge financial support from the Engineering and Physical Sciences Research Council (EPSRC; Grant Nos EP/H024107/1, EP/I033459/1, EP/J00135X/1, EP/J015156/1, EP/K021966/1, EP/K023004/1, EP/K038885/1, EP/L015668/1 and EP/L023652/1), and the European Research Council (ERC; project 670467 SMART-POM).

Competing interests statement

The authors declare no competing interests.

Publisher's note

Springer Nature remains neutral with regard to jurisdictional claims in published maps and institutional affiliations.

How to cite this article

Vilà-Nadal, L. & Cronin, L. Design and synthesis of polyoxometalate-framework materials from cluster precursors. *Nat. Rev. Mater.* **2**, 17054 (2017).

DATABASES

Inorganic Crystal Structure Database: <https://cds.dl.ac.uk/cds/datasets/crys/icsd/llicsd.html>